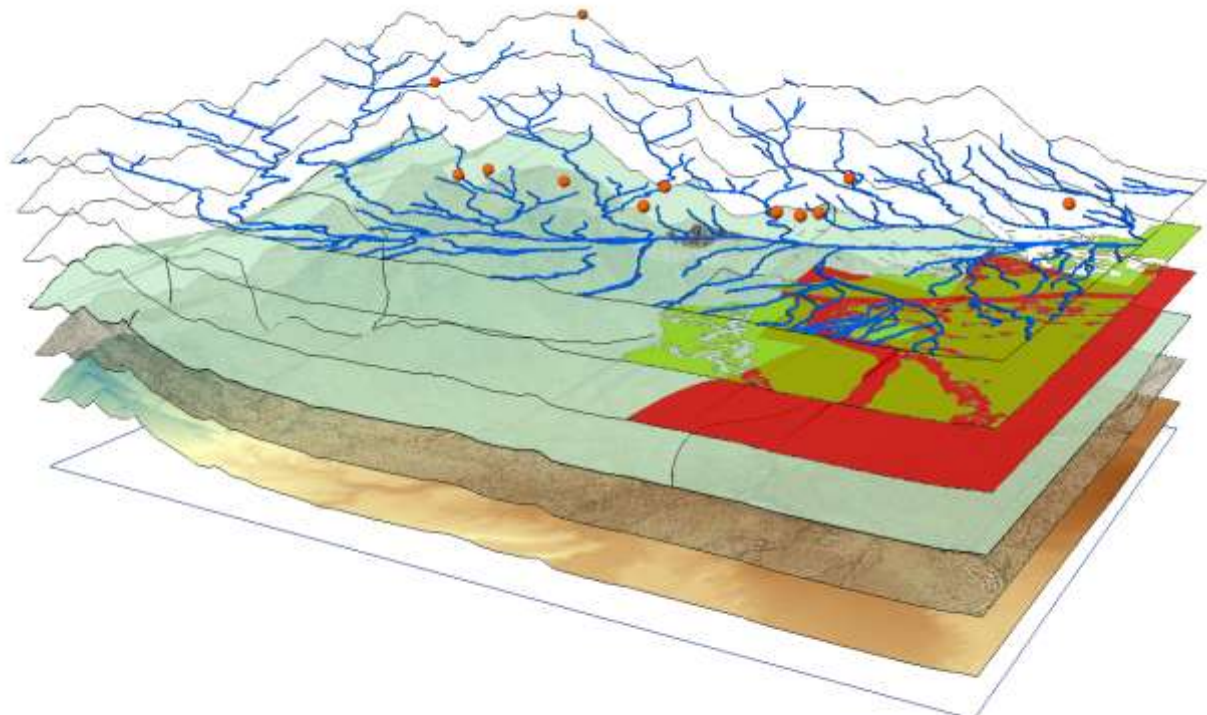




UNIVERSITY *of* PORTSMOUTH

Practical Portfolio 1

Using GIS for Geographical Analysis



Contents:

1.0	An Evaluation of QGIS	3
2.0	Network Analysis: Glass Recycling Banks	6
2.1	Recycling Bank: Point 1:.....	8
2.2	Recycling Bank: Point 2:.....	9
2.3	Recycling Bank: Point 3:.....	10
2.4	Recycling Bank: Point 4:.....	11
2.5	Recycling Bank: Point 5:.....	12
2.6	Final advised distribution of Glass Recycling Banks	13
3.0	Multi-Criteria Terrain Analysis.....	14
3.1	Methodology	14
3.1.1	Viewshed Tool: 'Not within view of any known observation point'	15
3.1.2	Slope analysis Tool: '< 14 degrees slope'	15
3.1.3	Buffer zones: 'Avoid urban areas by at least 2km'	16
3.1.4	Topological Overlay: 'Road buffer to road polygon'	16
3.1.5	Data conversion: 'Polygon to raster'	17
3.1.6	Reclassification tool: 'Classification of raster outputs'	17
3.1.7	Raster Mathematical Operations: 'Boolean Algebra for HLZ'	18
3.2	Limitations	18
3.3	Operation Brown Trousers: Briefing Map 1 showing HLZ.....	19
4.0	ArcPy Python Programming: An Introduction	20
4.1	Digimap file batch import and conversion.....	20
4.2	Processing raster information into Boolean raster	21
4.3	Batch processing python script.....	22
4.4	Complex operations: Brown Trousers	23
5.0	Assessing land cover change: Mato Grosso, Brazil.....	24
5.1	Introduction	24
5.1.1	Vegetation clearance in Mato Grosso, Brazil	24
5.1.2	Remote sensing: Tool for land cover change analysis.....	24
5.2	Study Topic and Methodology.....	24
5.2.1	Mato Grosso	24
5.2.2	Data Source.....	24
5.2.3	Analysis Method	25
5.3	Results	37
5.3.1	NDVI.....	37
5.3.2	Highlight Change	37
5.3.3	Land Cover Change – Thematic Maps	37
5.4	Discussion	38
5.4.1	Limitation.....	38
5.5	Conclusion	39
6.0	Land Surveying of Portland Building, Portsmouth.....	40
7.0	Bibliography.....	42
7.1	Literature:.....	42
7.2	Images:	43

1.0 An Evaluation of QGIS

Initially QGIS 2.8.2 GUI is different from the ArcGIS however it does have themes of the standard running through it. It makes good use of the horizontal toolbar, while also introducing the new vertical toolbar incorporated with the standard layer view menu.

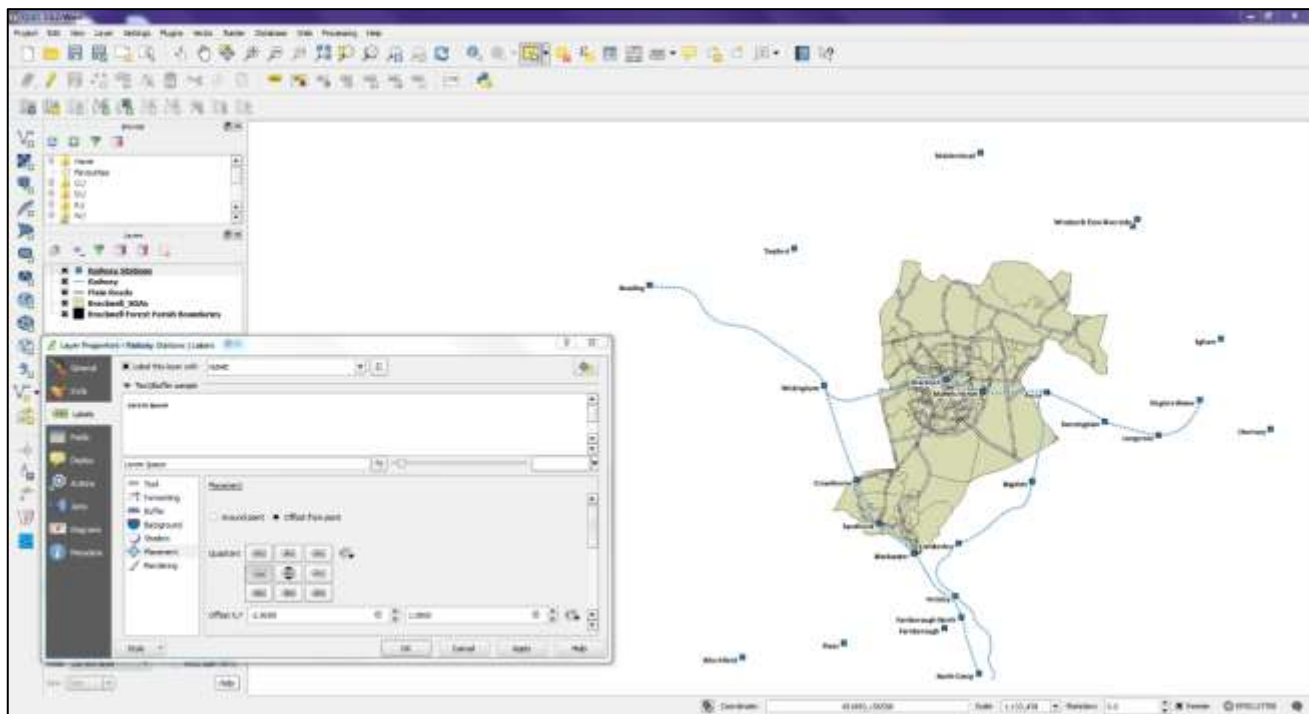


Figure 1.0: A screenshot, showing the initial stages of processing and map customisation, which includes the text placement customization. Unfortunately you are unable to give individual labels differing placements, therefore the stations Windsor & Eton Riverside and Central, overlap and at certain scales you unable to see the Central station.

The Picture below illustrates how QGIS offers more options if you edit layers via the layer drop down menu from the top tool bar, previously I couldn't filter out road name labels however using layer labelling settings I was able to.

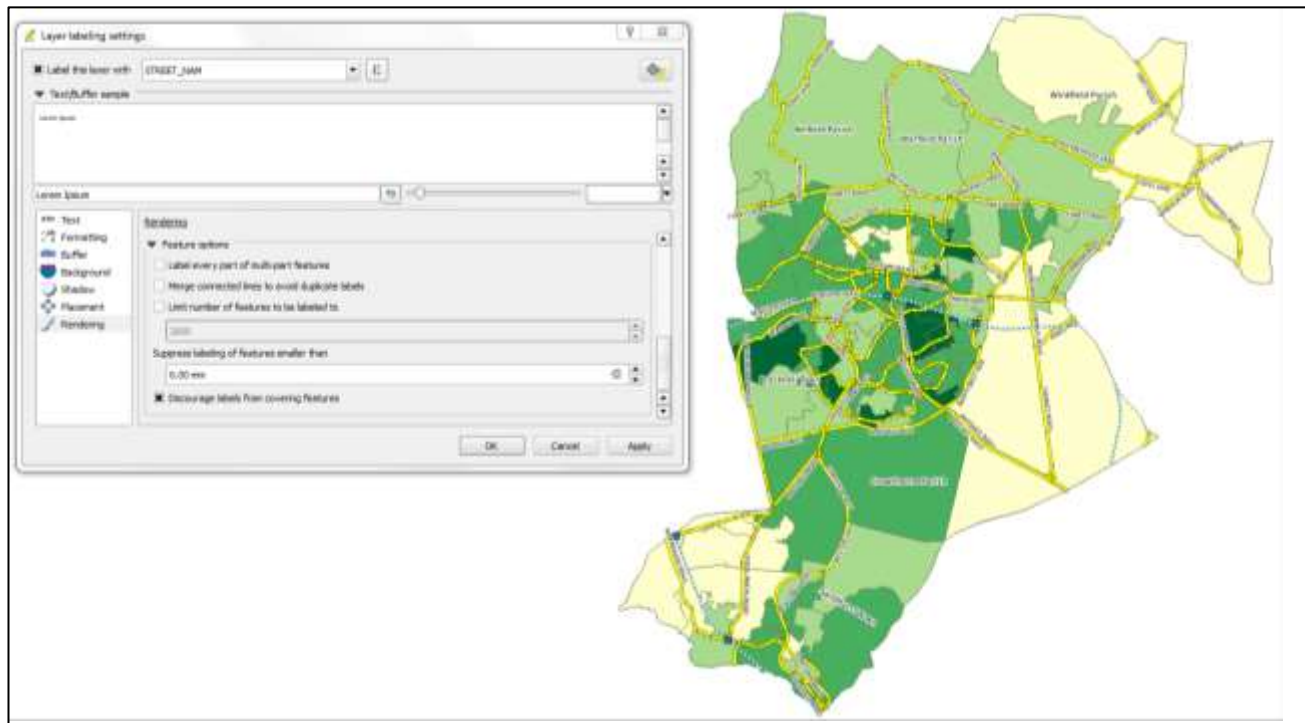


Figure 1.1: A screenshot, showing the advanced ability to further editing layer labelling settings via the horizontal tab toolbars.

The next area of investigation was heat mapping. In comparison to ArcGIS's toolbox and spatial analyst approach, QGIS follows the more symbolic style of tool bar again with clear defined options. Below is the sort of product possible.

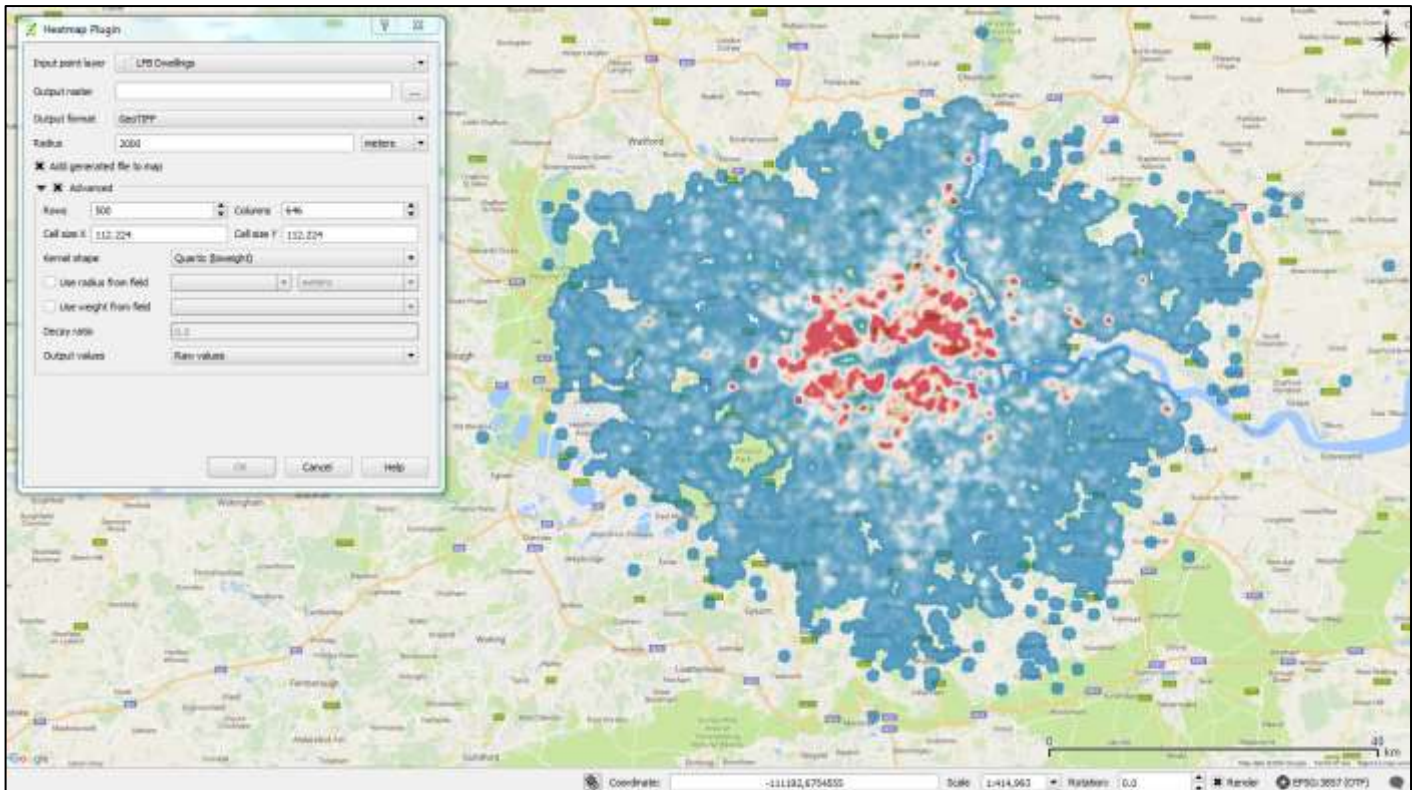


Figure 1.2: Above is a view of what is possible with heat mapping on QGIS, the map shows incidents in dwellings, as recorded by the London Fire Brigade. Again the categorised colouring was done using the style tab in the layer properties.

The process of creation was no more than two steps, whereas ArcGIS feels more technical using the toolbox approach and various parameters such as point, line and kernel density. This theme is common in most QGIS processes.

The plug-in menu is another feature that differs from ArcGIS, it enables both popular and new 3rd party plug-ins to be installed and used inside QGIS, and this opens QGIS's boundaries. It enables anything a 3rd party can create for their particular need from a GIS. Here it was used to enable open source base maps such as Google Streets, to the right is a view of the plug-in menu's features.

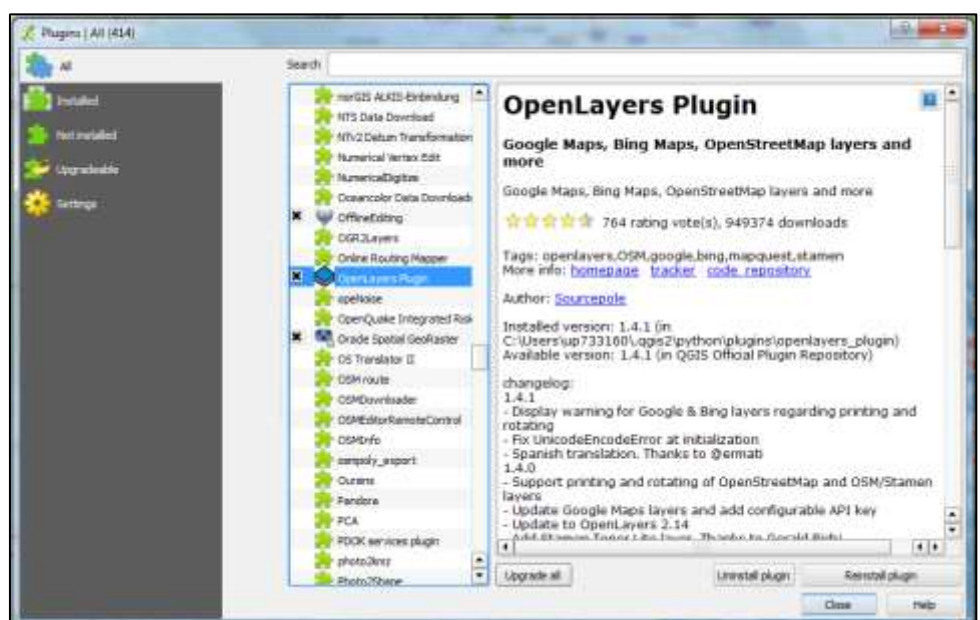


Figure 1.3: Here is a view of the Plug-ins menu, the settings tab enables new plugin app repository's to be added, enabling 3rd party plug-ins.

The QGIS composer feature which is similar to ArcGIS's Layout view, is limited, again its the usual 'simple symbol' QGIS theme, however some features are missing, and the scale bar is very difficult to make sense of.

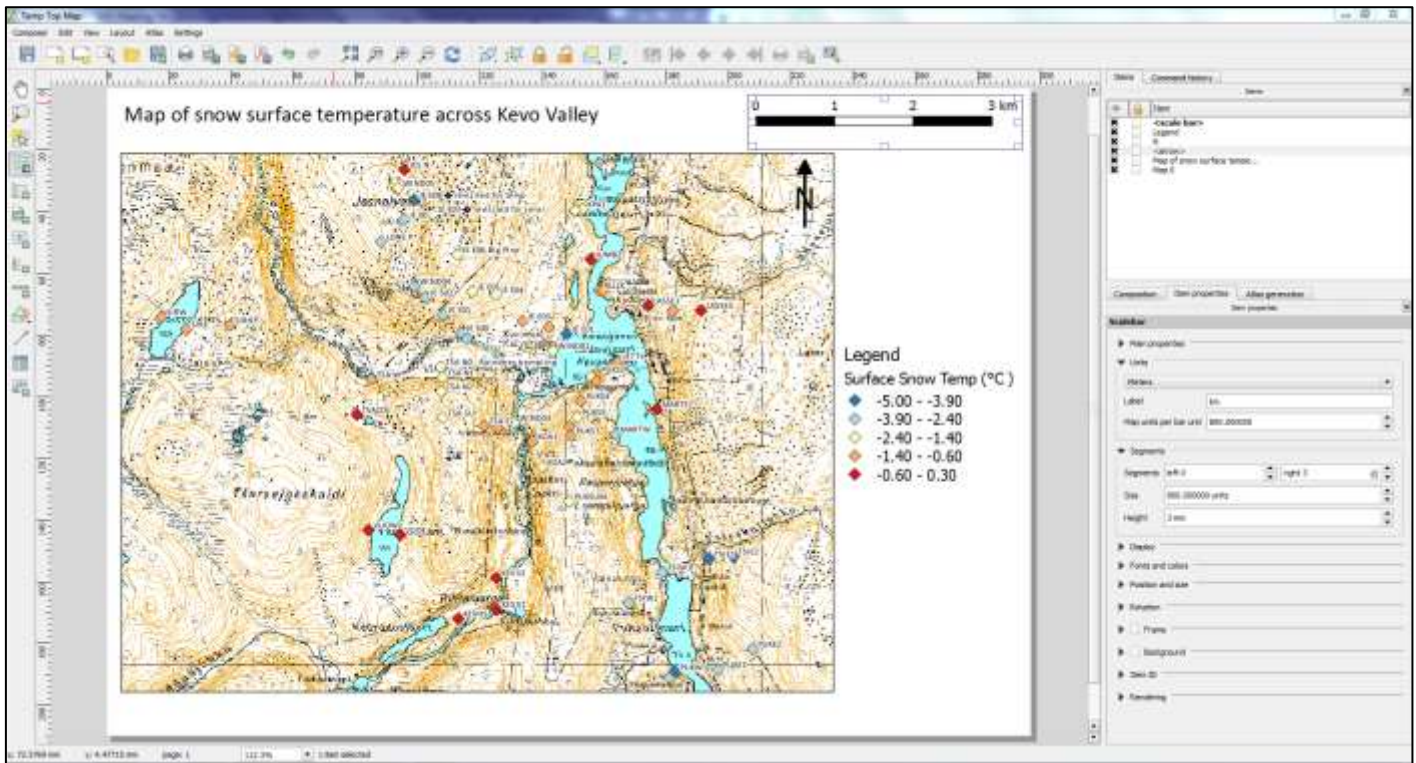


Figure 1.4: Above is a map containing surface snow temperature for a valley system in Finnish Lapland, taken from field data collection. The scale bar seems to have no continuity with the map, this is a common issue raised by the online community, and the best outcome is to align and manipulate it to a known graticule.

To summarise, QGIS has a simpler GUI and is more user friendly, functions well as a program, and has options for 3rd party expansion. However I feel it could limit a learned user of GIS, and still needs development in the composer section. While there are shortfalls with QGIS, it is not a polar opposite from other software, and as suggest by a review from Maurya et al (2015), the quality is closer than profit based companies would like to admit.

2.0 Network Analysis: Glass Recycling Banks

This task requires the undertaking of network analysis “one of the most significant and persistent research areas in GIS” (Curtin, 2007) to assess the spatial variation of glass recycling banks across Portsmouth, and where, if given the chance, we would put 5 new glass recycling banks. Below is a map showing the current distribution. The current amount of households covered is 45,817 out of 88,399, or 51.8%. The current coverage of banks shows a wide coverage on the island with a focus on Southsea, and disparities in both Cosham and North end. This may be due to lower population density figures, however Cosham does seem particularly underrepresented.

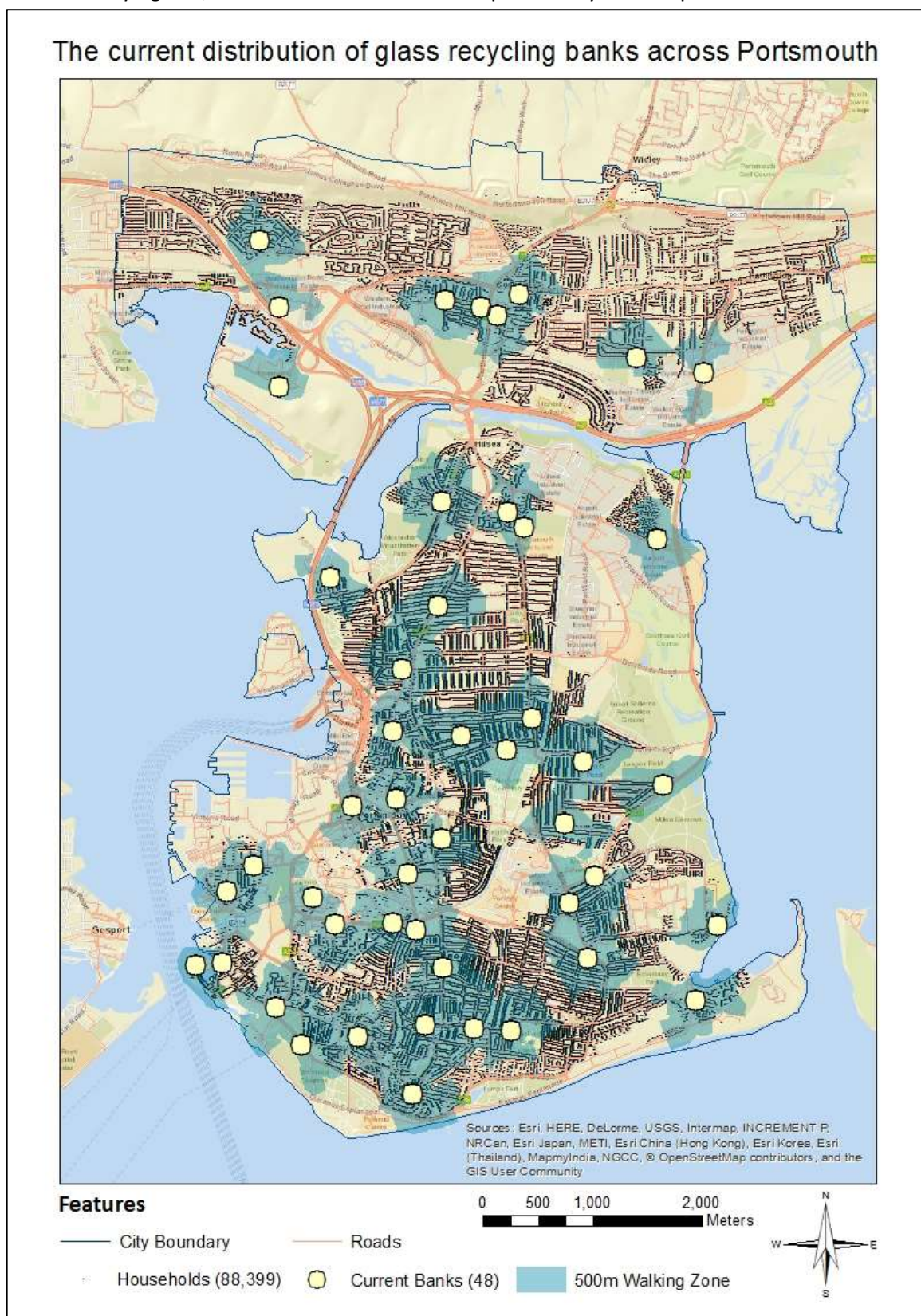


Figure 2.0: Map showing the original dataset spread of recycling banks across Portsmouth.

Data Source: Contains OS data © Crown copyright and database right (2014), Portsmouth City Council (2015), Google Maps & Street View (2016).

I then realised the data set provided needed updating with current recycling banks, newly installed. Here is the resulting map. This newly updated map of current banks gives a household coverage of 50,350 out of 88,399, or 57%. This is an increase of 5.2%.

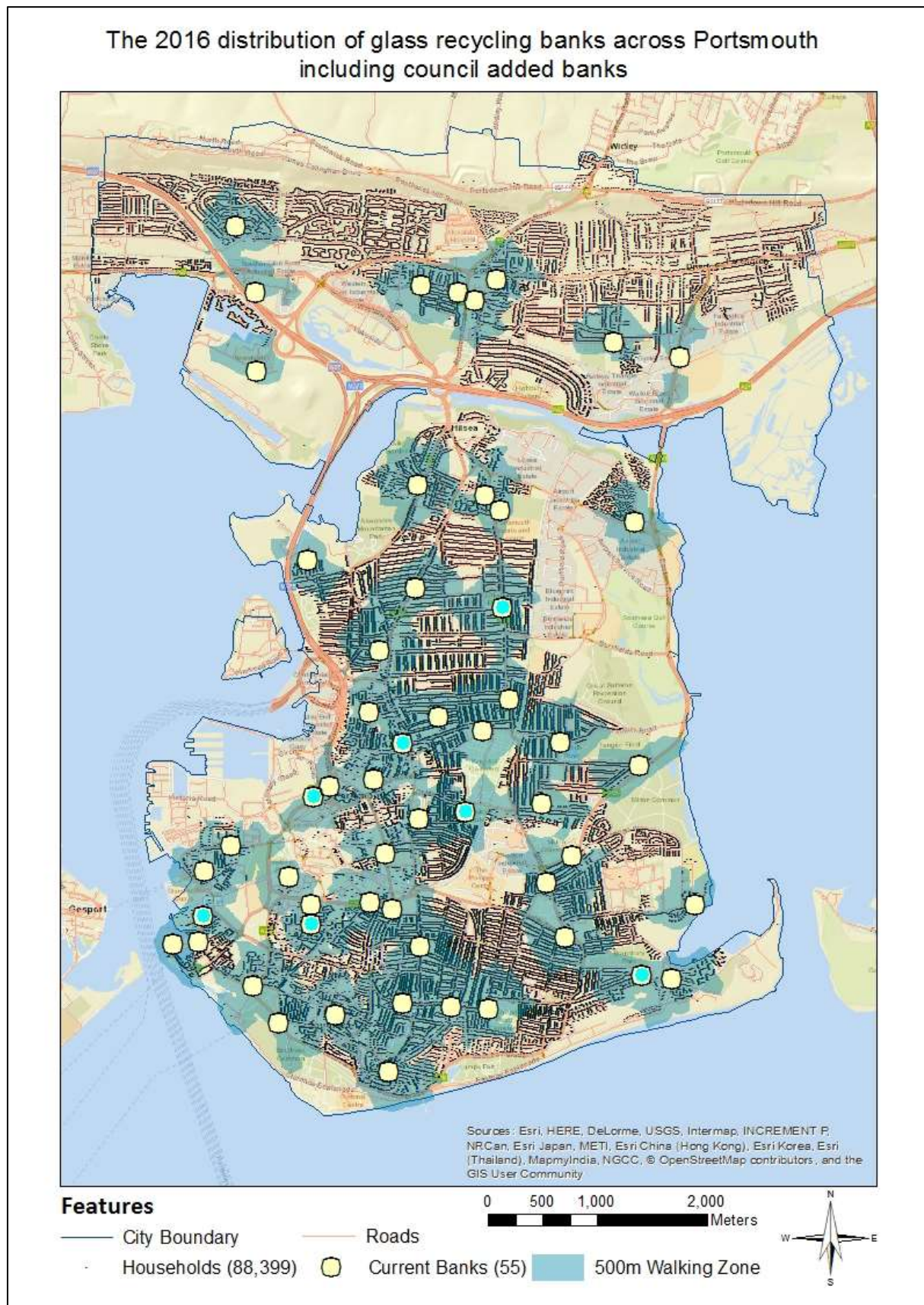


Figure 2.1: Above is a map showing the current points as up to date with the council recycling website, www.recycle-more.co.uk. The points highlighted in blue are the newly added points.

Data Source: Contains OS data © Crown copyright and database right (2014), Portsmouth City Council (2015), Google Maps & Street View (2016).

2.1 Recycling Bank: Point 1:

The first point of new bank placement was at a commercial 'Spar' corner shop alongside a current clothes bank at Devonshire Avenue. An updated coverages shows an increase of 2,026 households to 52,376 from this bank, a rise of 2.2%.

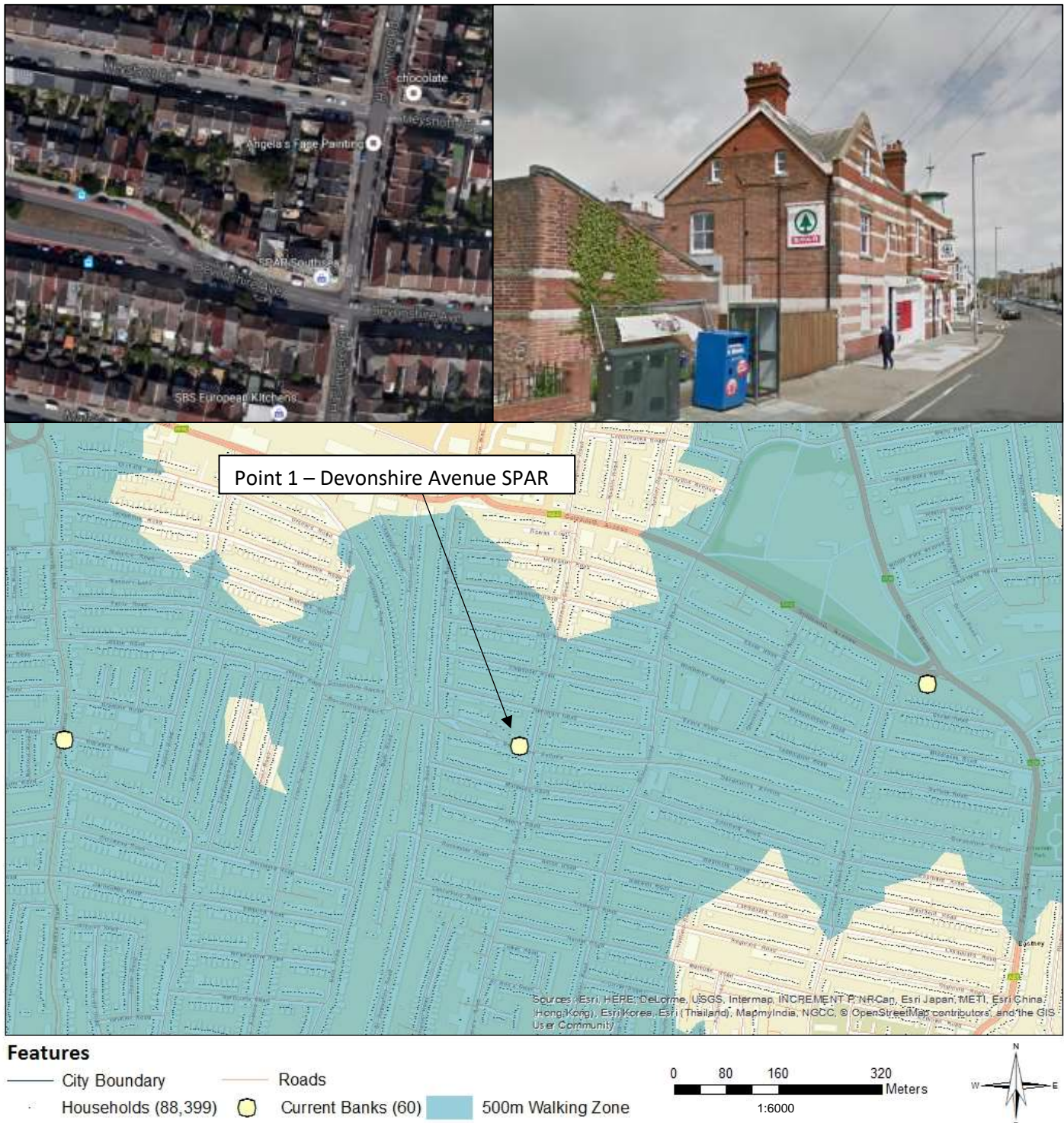


Figure 2.2: Image shows the placement of point 1, placement was decided on proximity to vulnerable areas, it is outside a commercial property, and would be placed alongside a clothes bank. It is convenient for local residents and also it's over 300m from the closest school. Data Source: Contains OS data © Crown copyright and database right (2014), Portsmouth City Council (2015), Google Maps & Street View (2016).

2.2 Recycling Bank: Point 2:

The second glass recycling bank placement will be on the Tesco forecourt. This gives a new coverage of 53,287 and increase of 911, 1.0%.

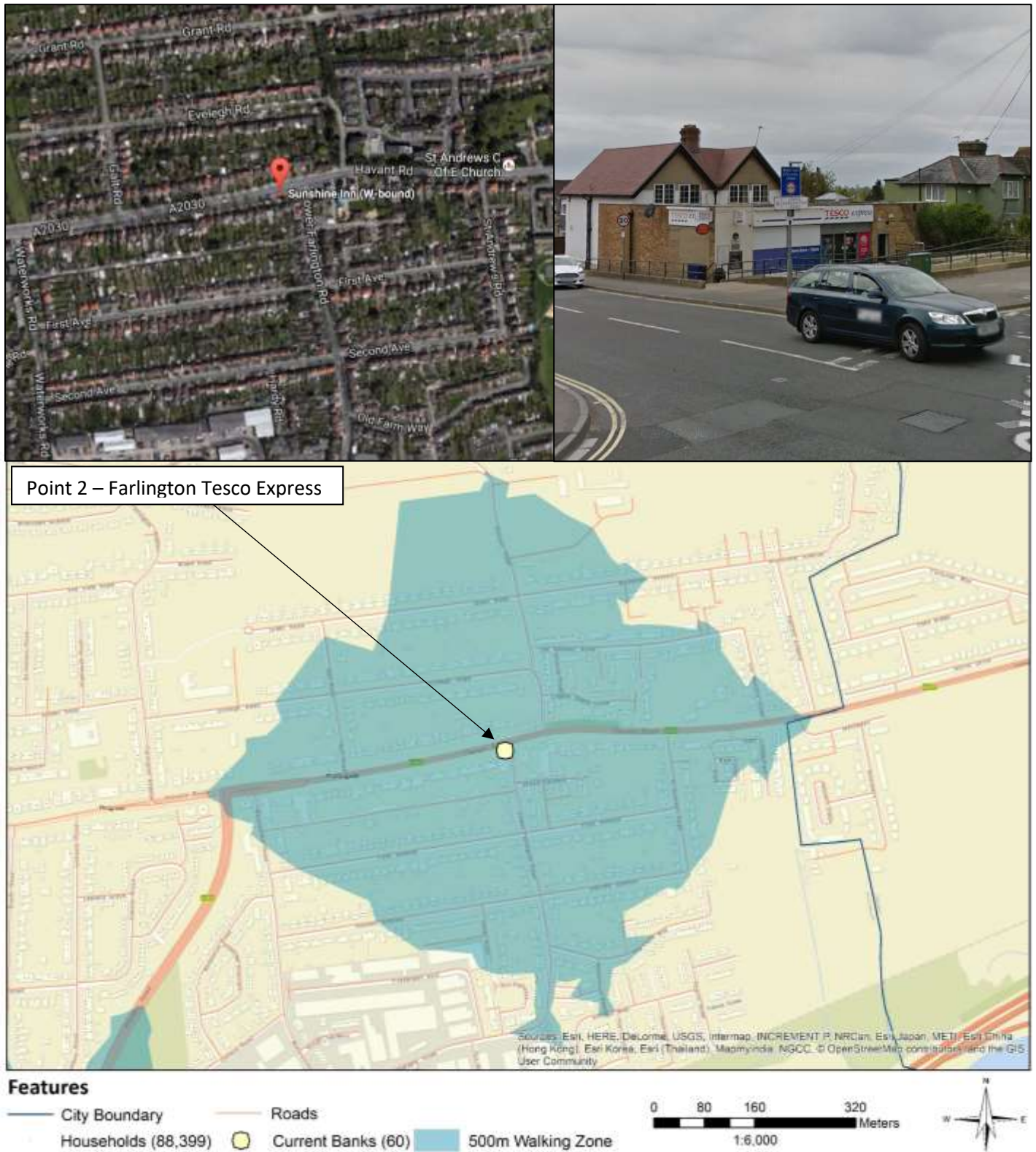


Figure 2.3: Image shows the placement of point 2, it is at a commercial hub just on the Tesco express forecourt. Therefore it is convenient for local residents. It is opposite a pub which I would assume produces a lot of glass waste and could make use of this facility.

Data Source: Contains OS data © Crown copyright and database right (2014), Portsmouth City Council (2015), Google Maps & Street View (2016).

2.3 Recycling Bank: Point 3:

The third recycling bank was placed at the ‘best one’ Corner shop forecourt, there is enough space there and the location is very central to the rest of the residential area from Kirby Rd to Chichester Rd. This gives an updated coverage of 55060, an increase of 1,773 or 2.0%.

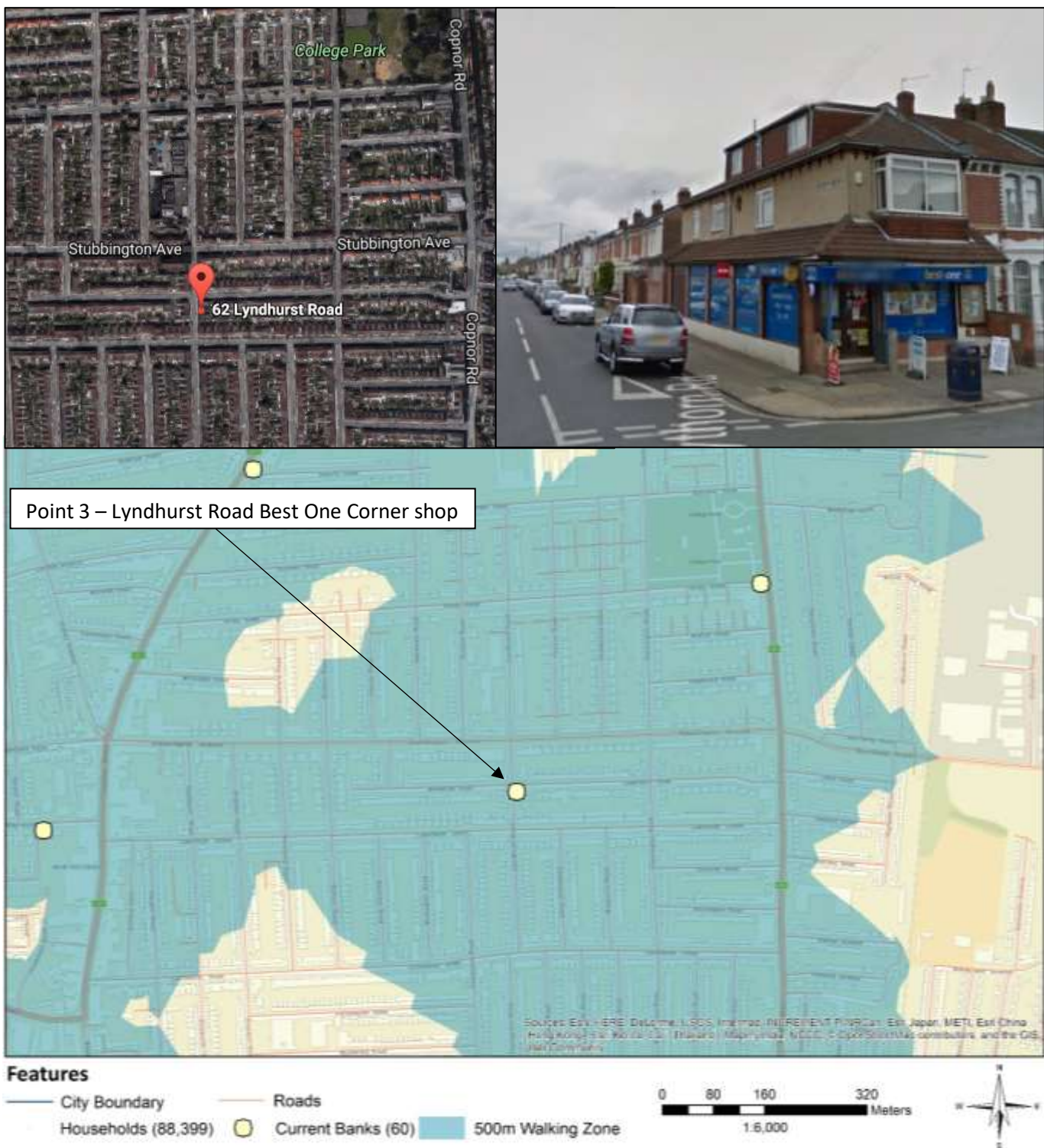


Figure 2.4: Image shows the placement of point 3, it is among a densely populated terraced estate. However due to the placement on a commercial forecourt it will not be in direct proximity of residential housing. This will allow for proper and full use while not being an inconvenience with regards to noise.

Data Source: Contains OS data © Crown copyright and database right (2014), Portsmouth City Council (2015), Google Maps & Street View (2016).

2.4 Recycling Bank: Point 4:

The penultimate bank is best placed off of the B2154 Eastney roundabout between the Henderson Rd and A288 exit. This placement will give an update coverage of 56,869 households and increase of 1,809 or 2.0%.

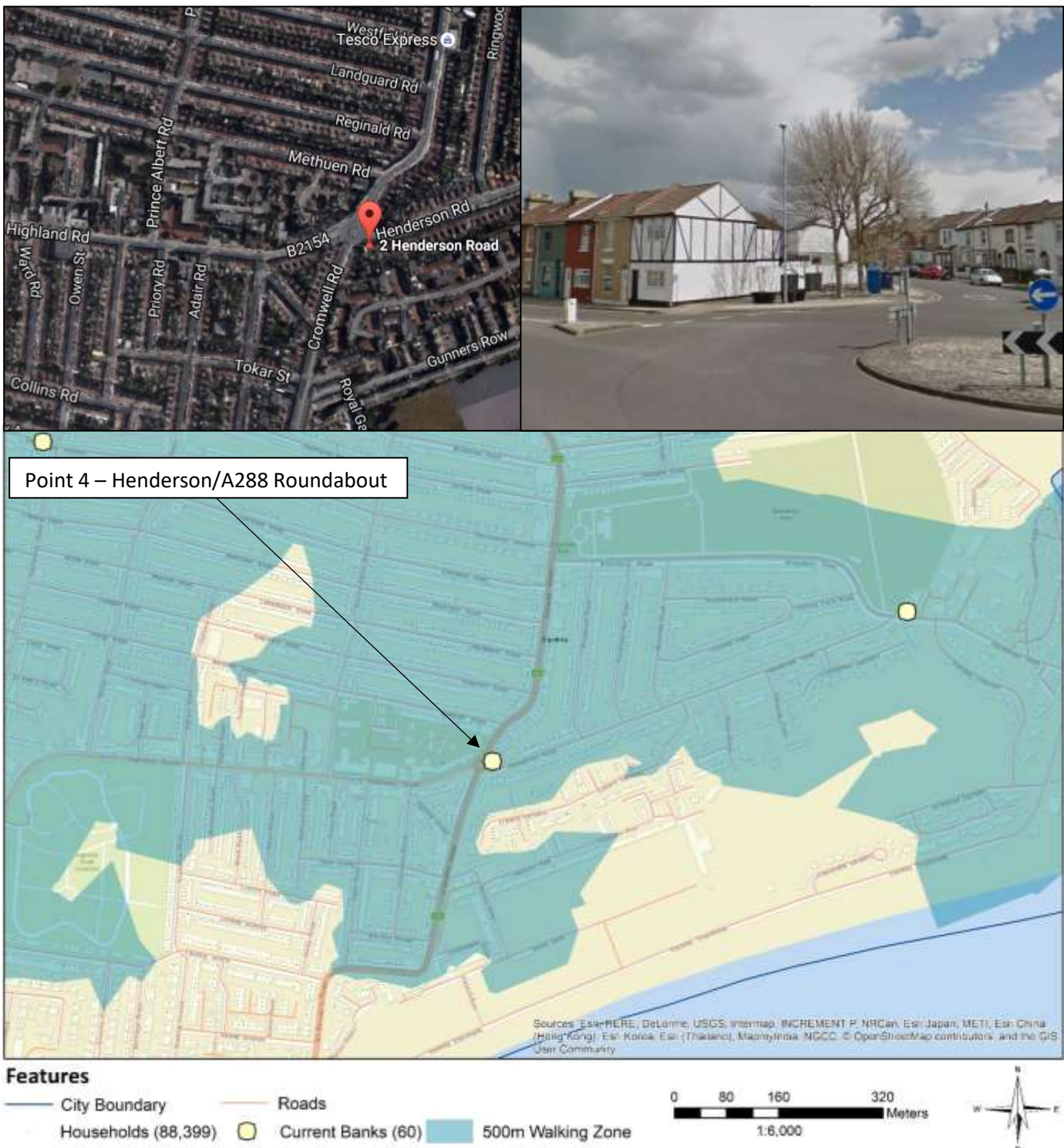


Figure 2.5: Image shows the placement of point 4, it is towards the southeast coastal area of the island, Eastney. There is already a large clothes bank in this space, and as before a glass recycling bank could place well alongside.

Data Source: Contains OS data © Crown copyright and database right (2014), Portsmouth City Council (2015), Google Maps & Street View (2016).

2.5 Recycling Bank: Point 5:

The final point that would be most suited to a new recycling bank would be near the Blakemere Crescent bus stop in Cosham, giving an increase household coverage to 57,949 and increase of 1,080 on the last, or 1.2%.

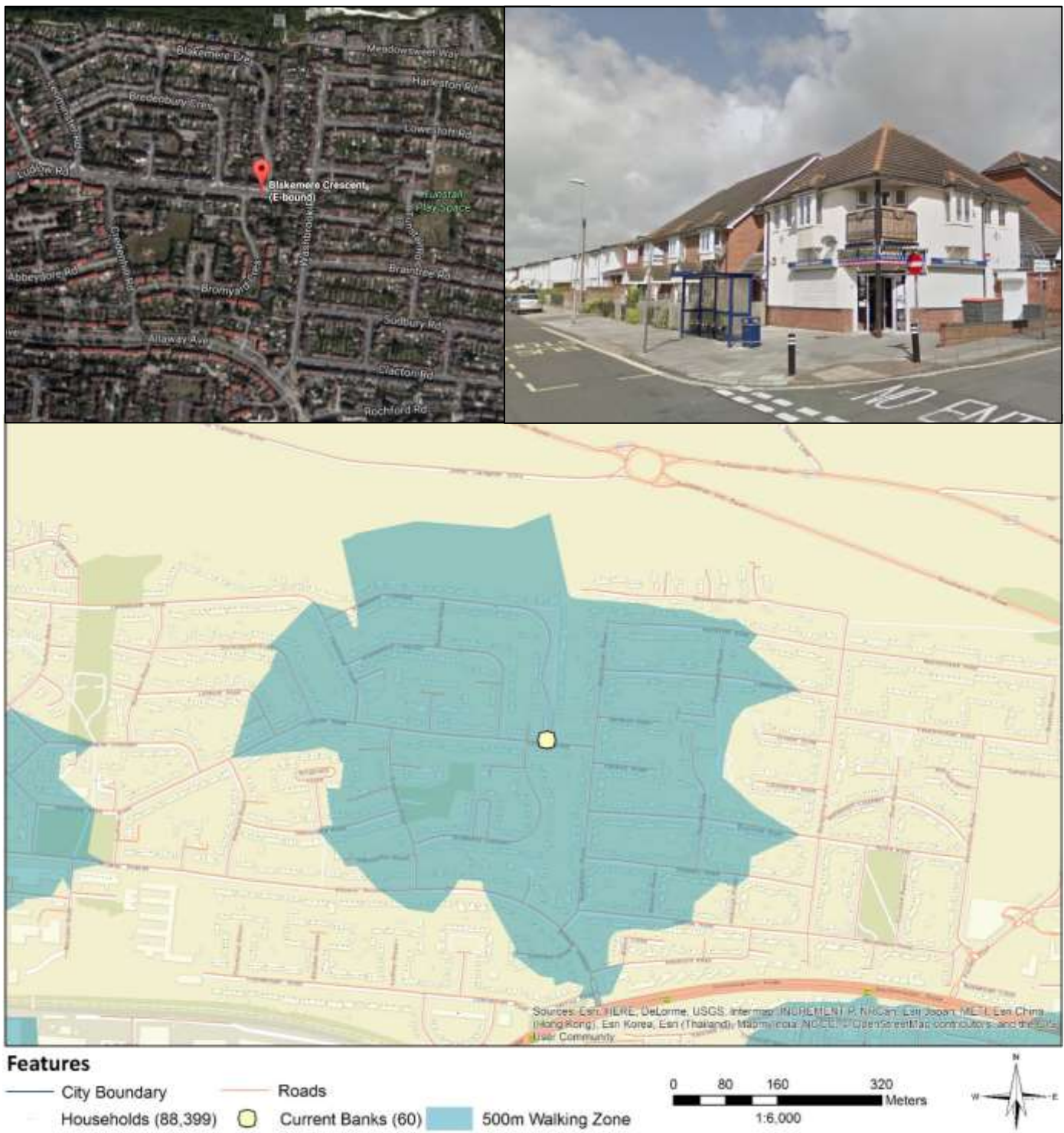


Figure 2.6: Image shows the placement of point 5, this point is near a commercial area buried within a residential setting for local convenience.

Data Source: Contains OS data © Crown copyright and database right (2014), Portsmouth City Council (2015), Google Maps & Street View (2016).

2.6 Final advised distribution of Glass Recycling Banks

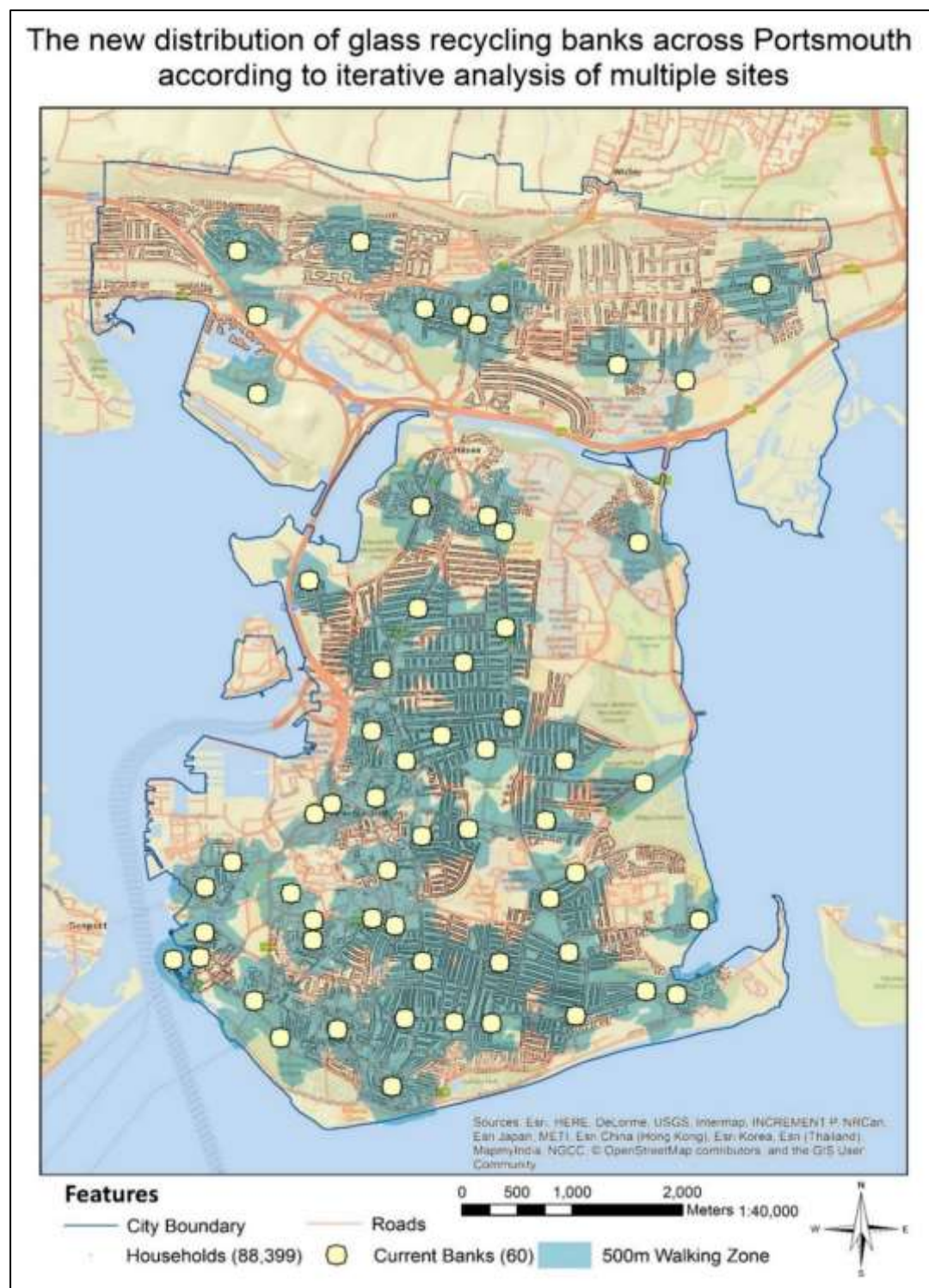


Figure 2.7: Final map showing placements of the 5 newly advised Glass Recycling Bins.
Data Source: Contains OS data © Crown copyright and database right (2014), Portsmouth City Council (2015), Google Maps & Street View (2016)

The newly advised distribution with updated 2016 current bank distribution including 5 more advised points. Together this gives a total coverage of 57,949 (65.6%) which is an increase of 12,131 (13.7%) from the original data set or an increase of 7,599 (8.6%) from the current coverage. It is important to recognise the distribution disparities across the island and Cosham, the denser island areas give a higher increase due to density of people. Whereas only 20% of households in Portsmouth are in Cosham, and therefore there is a sparser household spread, meaning coverage per bank is lower. This has been considered in the newly advised banks which brings the amount of banks in Cosham to 18% of overall banks across Portsmouth and therefore more in line with the population spread.

3.0 Multi-Criteria Terrain Analysis

This task takes a fictitious scenario and requires toolbox functions to create separate raster Boolean layers and finally combine them to allow the correct aims to be met. This in turn results in figure 3.3 a detailed map with the required information processing to give safe landing zones. This type of analysis is commonly used within studies and real life events as shown in articles by Rikalovic et al (2014), Kallali et al (2007) and Rybarczyk and Wu (2010).

3.1 Methodology

A variety of steps were used to create 7 necessary Boolean layers. Below in figure 3.1 is an overview of the processes used for the final production of figure 3.3.

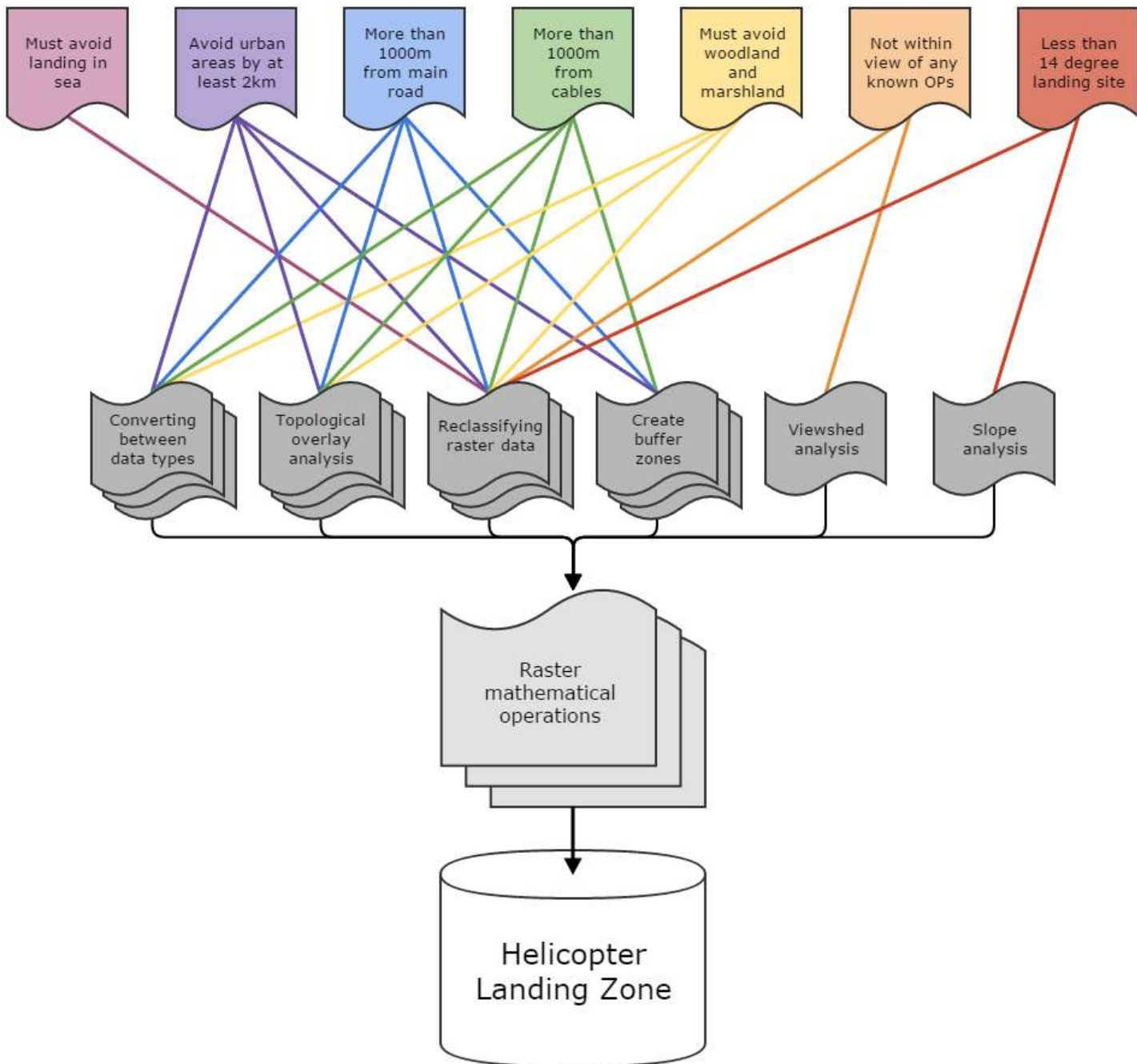


Figure 3.1: Flow diagram of processes used for final raster creation.

3.1.1 Viewshed Tool: 'Not within view of any known observation point'

Initial input here was a raw altitude DTM and known observation points, after viewshed analysis had processed what cells could be seen by the one or more points and numbered them accordingly, it colour codes them as below. Where 0 equals green, 1 is pink, 2 is red, 3 is turquoise and 4 is purple.

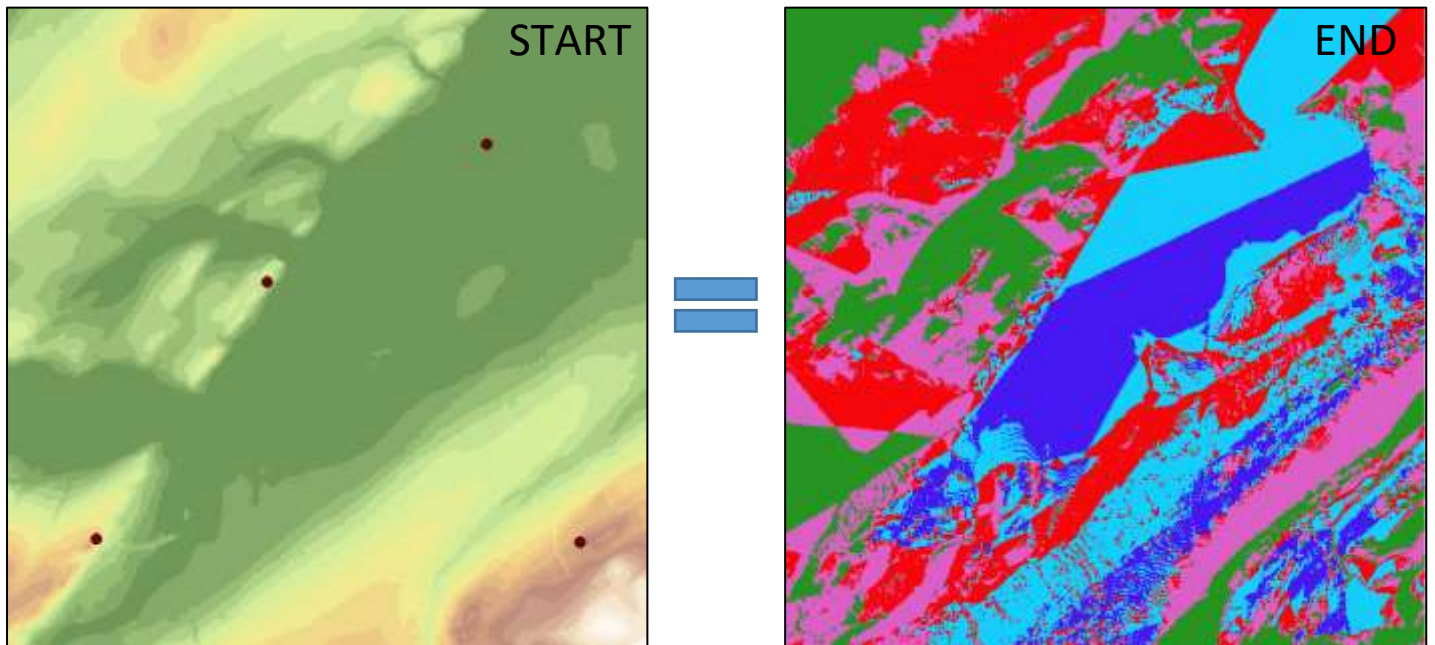


Figure 3.1.1: Viewshed analysis process from altitude raster and observation points to viewedshed layer.

3.1.2 Slope analysis Tool: '< 14 degrees slope'

Slope analysis tool uses a differentiation algorithm to calculate maximum rate of change between cells and their neighbours. The result is a classified output of areas equal and above (white) 14 degrees and below 14 degrees (green).

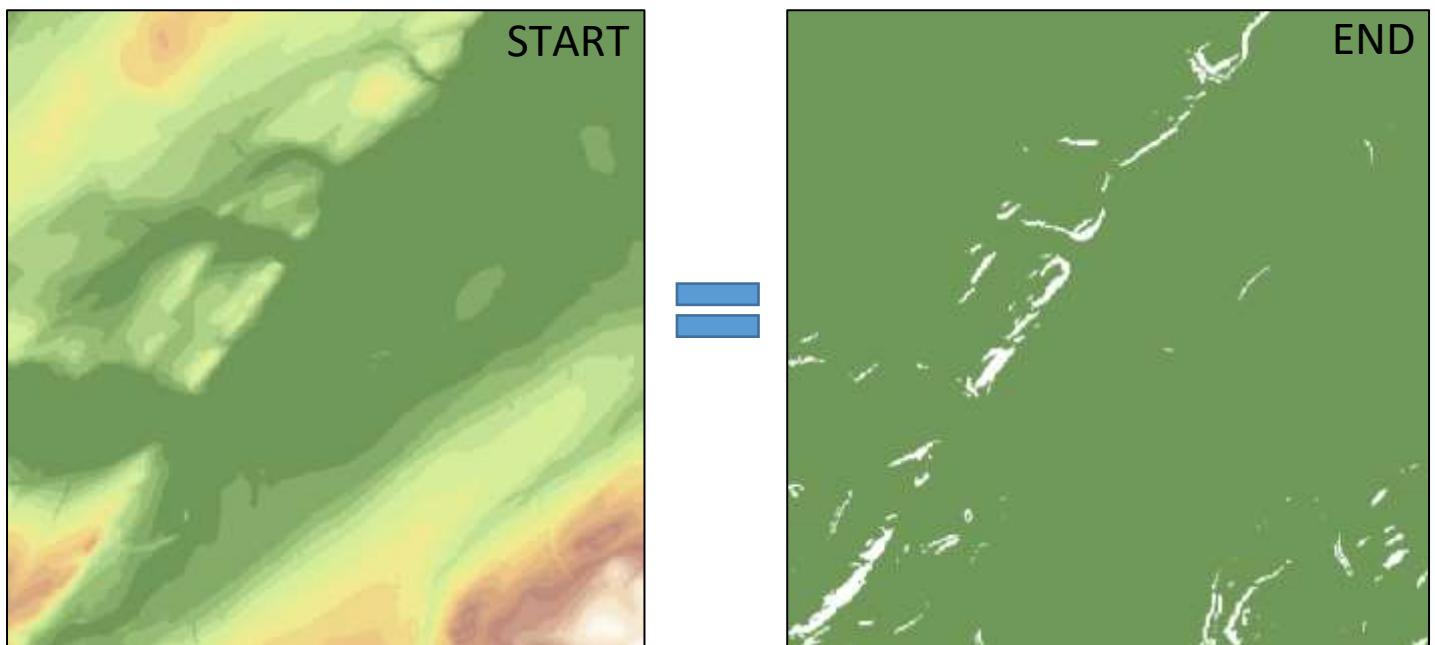


Figure 3.1.2: Slope analysis process from altitude raster into slope raster.

3.1.3 Buffer zones: 'Avoid urban areas by at least 2km'

This stage takes the polygon input and creates buffer zones of a set distance around features, creating a buffer polygon.

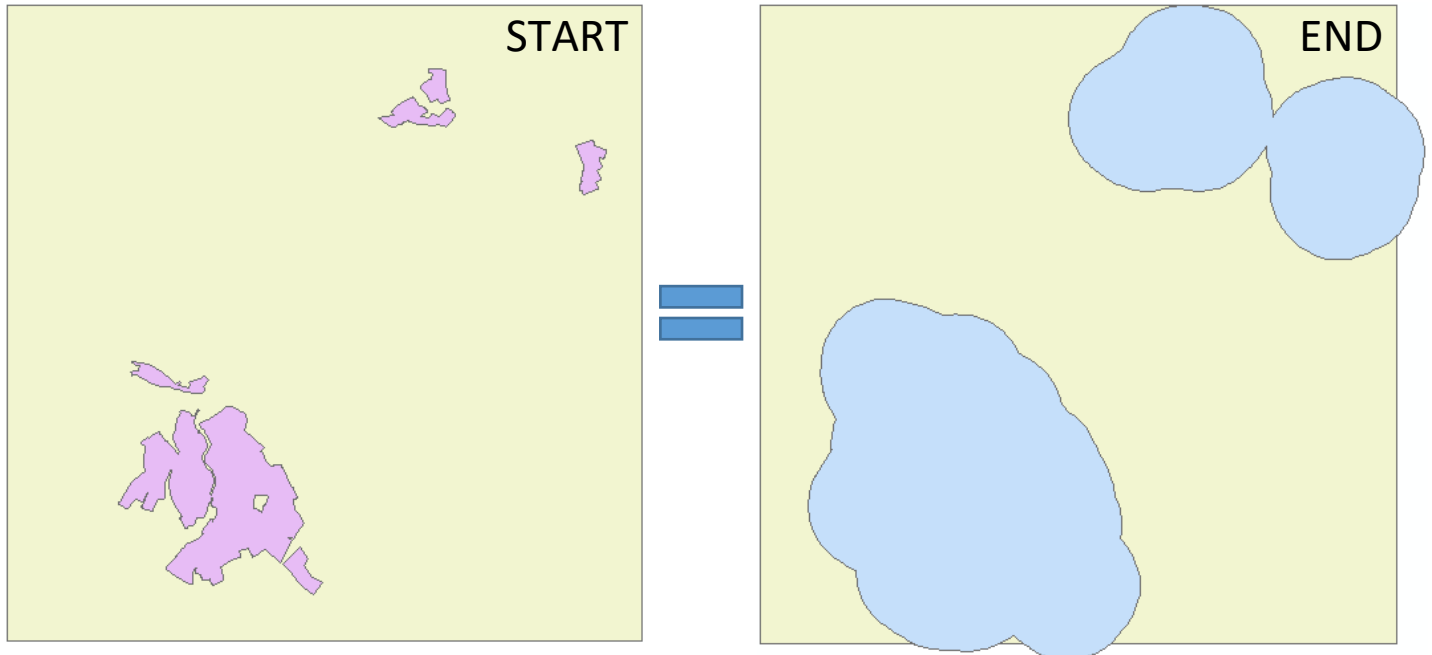


Figure 3.1.3: Buffer zone processing from urban polygon to urban

3.1.4 Topological Overlay: 'Road buffer to road polygon'

This uses the identity overlay to take the map box (yellow) input and combine with identity feature (green) leaving all feature within input, merged into the final polygon form.

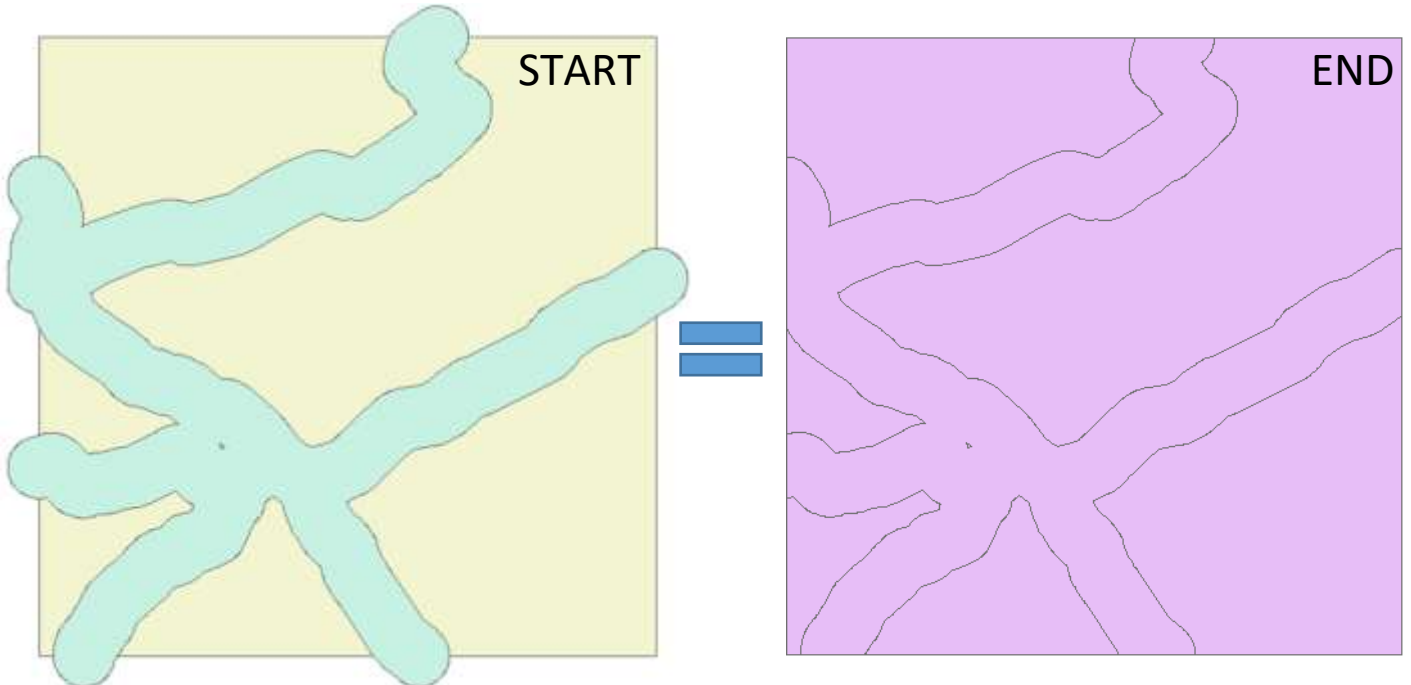


Figure 3.1.4: Overlay processing of the road buffer to a final overlay polygon.

3.1.5 Data conversion: 'Polygon to raster'

This tool simply converts polygon to raster, with a cell size of 20. The resultant raster is necessary for Boolean algebra whereas polygon would have been inappropriate.

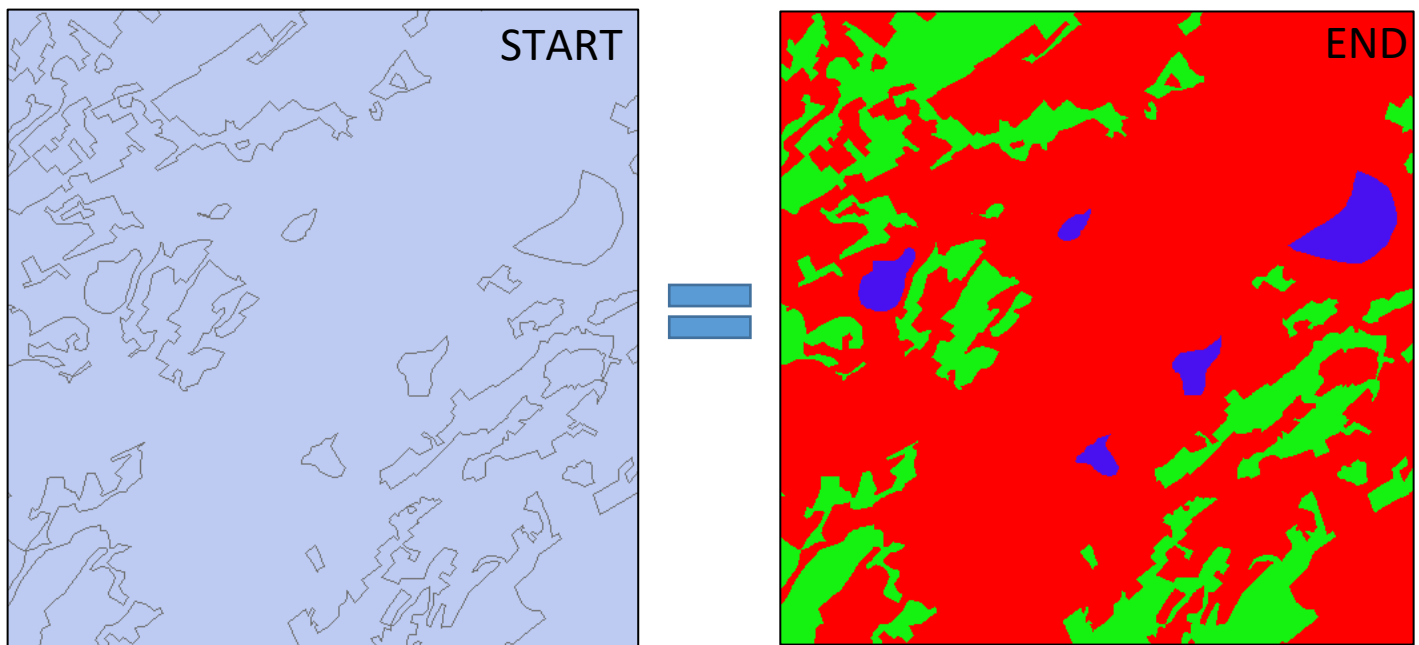


Figure 3.1.5: Data conversion process from polygon to classified raster layer.

3.1.6 Reclassification tool: 'Classification of raster outputs'

This classifies raster's into 1 and 0 where 1 meets our aims and 0 does not, as a result Boolean algebra is possible for all reclassifications.

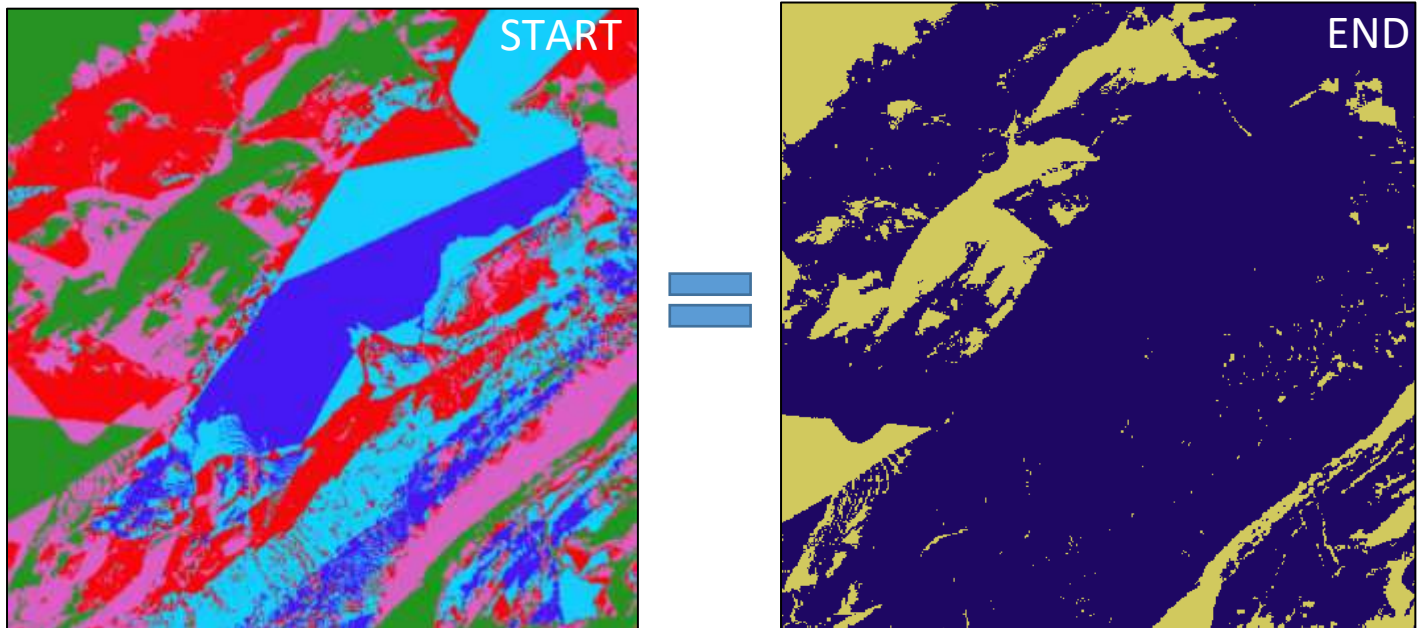


Figure 3.1.6: Reclassification process from many classes to just two, meets aims (1) or doesn't meet aims (0).

3.1.7 Raster Mathematical Operations: 'Boolean Algebra for HLZ'

This final step consisted of multiplying all the reclassified raster layers meeting our aims using the binary coding method together. Producing a final raster layer of possibly drop zones for the helicopter, where 1 (blue) is a drop zone and 0 (grey) is not.

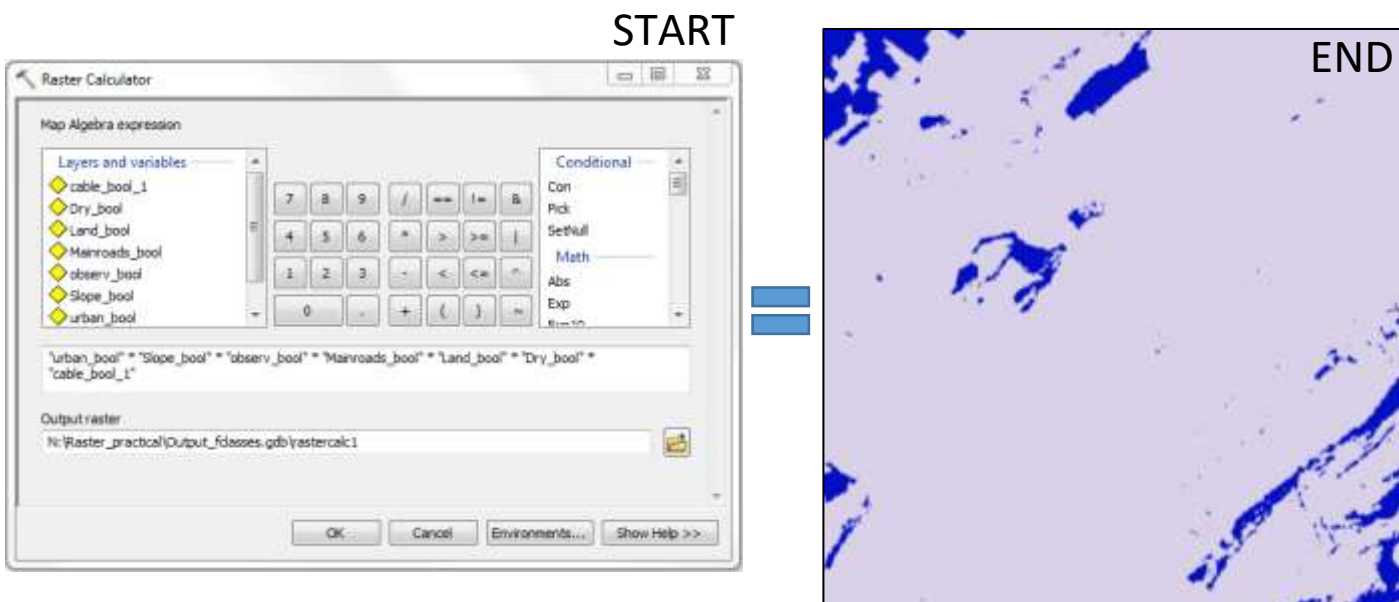


Figure 3.1.7: Raster mathematical process where all layers are combined to give the final product that meets the tasks aims.

3.2 Limitations

Multi-criteria analysis, while it does produce impressive results, that for this task completed the briefing, it does not come without limitations. The process is time consuming, the production of the end result can take up to an hour with over 7 final layers and even more within those. If map parameters are changed to meet a different need a whole repetition would be needed every time. The data was out of date with data from 2008/2010 terrain, this could have changed layers such as the coastline. As well as this the data source states the scale of the DTM is 200,000 whereas the task was to produce a 100,000 scale map. Both these source issues introduce inaccuracies across the map. Assuming the area was hand digitised, this introduces human error when it comes to land type boundaries etc. Lastly the process to create the sea level raster created a cut off at 0 where anything below this is classed as water and anything above was land. However this doesn't take into account areas that are below 0 but are still land, this may explain the inaccurate coastline.

In further literature a study by Hall et al (1992) also suggests limitations among Boolean multi-criteria analysis.



Figure 3.2: Coastline inaccuracies due to land classification.

3.3 Operation Brown Trousers: Briefing Map 1 showing HLZ



Operation Brown Trousers: Briefing Map 1

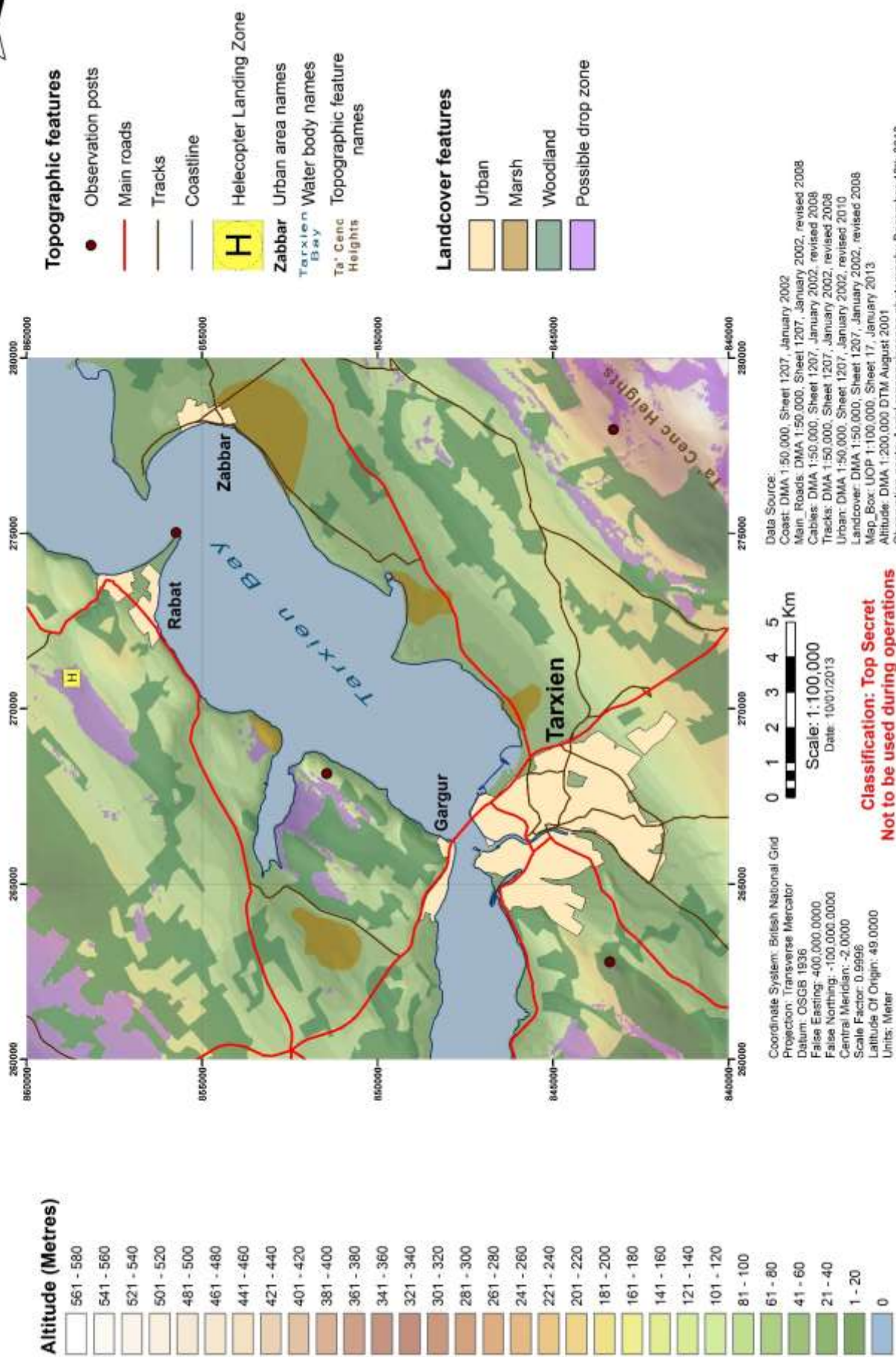


Figure 3.3: Operation Brown Trousers briefing map, showing suggested HLZ.

4.0 ArcPy Python Programming: An Introduction

Python has been described as the “programming language of choice” for ArcGIS by Zandbergen (2014). The reason for this is due to its simplicity and its accessibility as it is completely open source. Python also operates across platforms making it appropriate for all users, and a program like ArcGIS that is multi-platform. The code language itself is also interpreted meaning it will run directly from source code without compilation to binary, lastly the language is object oriented, which is exactly how ArcGIS is designed to work (Zandbergen, 2014). Python’s main task for ArcGIS is to automate workflow above and beyond a single user’s capabilities. (Jennings, 2011)

4.1 Digimap file batch import and conversion

Initial use of Python was to complete a bulk data import and conversion. The following code was run:

```
1. import os
2. import arcpy
3. arcpy.env.overwriteOutput=True
4. dir = arcpy.GetParameterAsText(0)
5. #Lists all individual directories in main data folder
6. for i in os.listdir(dir):
7.     #Joins file systems main directory and variable 'i'
8.     subdir = os.path.join(dir, i)
9.     #Picks just subfolders from the directory
10.    if os.path.isdir(subdir):
11.        #Lists all individual directories in subfolders
12.        for j in os.listdir(subdir):
13.            #Specifies input files from subfolders
14.            input = os.path.join(subdir, j)
15.            #Specifies output files from subfolders and what format you need them in
16.            output = os.path.join(dir, os.path.splitext(j)[0] + '.img')
17.            #Removes files first extension and replaces it with new specified extension
18.            if os.path.splitext(j) [1] == '.asc' :
19.                #Runs code in ArcMap
20.                arcpy.CopyRaster_management(input, output)
```

Figure 4.0: Digimap batch import and conversion python code, with green descriptors for how each line functions.

Next creation of a GUI was necessary to turn this script into an ArcMap tool. Once you’ve specified the required folder of files, results are similar to those shown below.

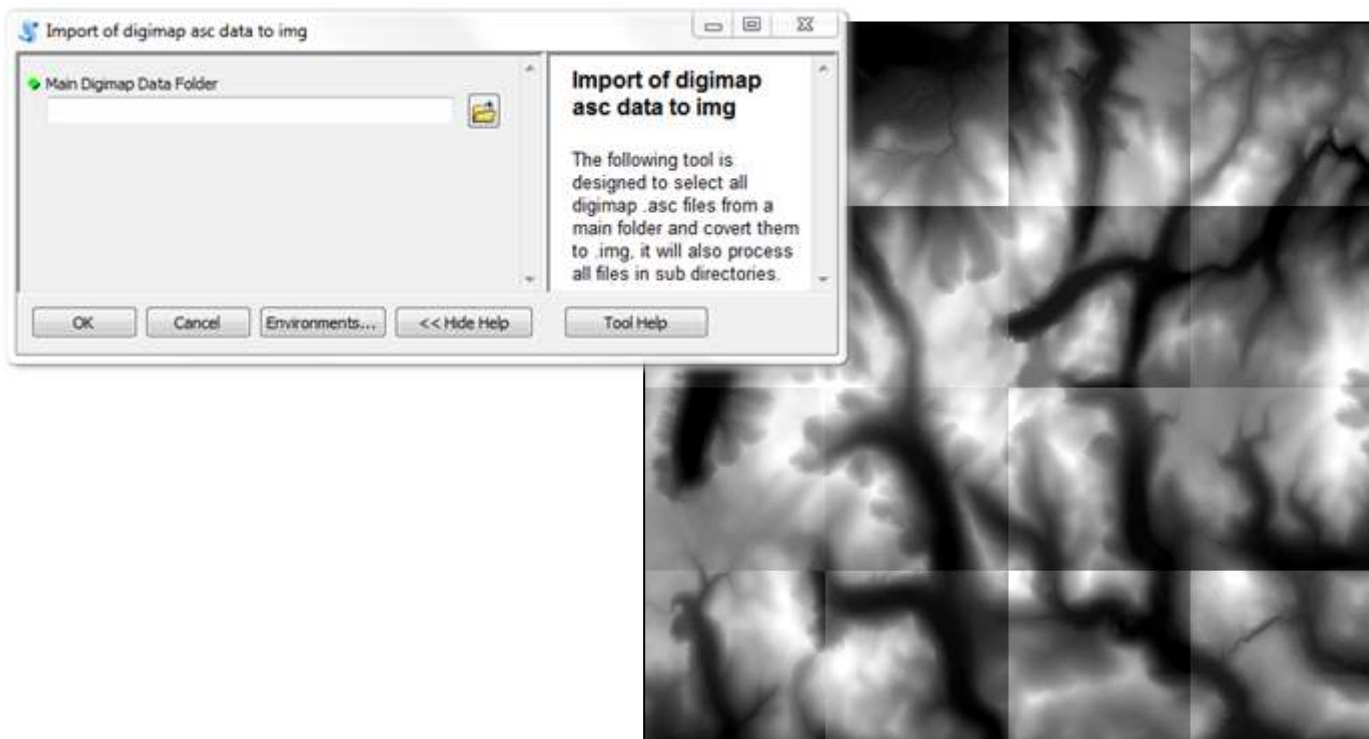


Figure 4.1: Digimap batch import and conversion python script, now with its own GUI for toolbox use. Resultant rasters as they appear in ArcMap.

4.2 Processing raster information into Boolean raster

The following code takes raster layers and specifies the areas above and below a certain height using a binary Boolean process.

```
1. #This script uses map algebra to find values in an
   elevation raster greater than a specified value.
2. import os
3. import arcpy
4. #Switch on the Spatial Analyst extension
5. arcpy.CheckOutExtension('Spatial')
6. #Load spatial analyst
7. #Specifies use of python within ArcMap or use of ArcPy tools
8. from arcpy.sa import *
9. #Specify the input/output raster
10. inRaster = arcpy.GetParameterAsText(0)
11. rasterOutput = arcpy.GetParameterAsText(1)
12. #Specifies numbers used are integers
13. cutoffElevation = int(arcpy.GetParameterAsText(2))
14. #Make a map algebra expression and save the resulting raster
15. #Specifies calculation used with chosen cut off elevation
16. outRaster = Raster(inRaster) > cutoffElevation
17. #Specifies output raster
18. outRaster.save(rasterOutput)
19. #Switch off Spatial Analyst extension
20. arcpy.CheckInExtension('Spatial')
```

Figure 4.2: Boolean raster creation for files allowing for specific elevation value (python code), with green descriptors for how each line functions.

Below is the resultant GUI and an example raster output for one file processed.

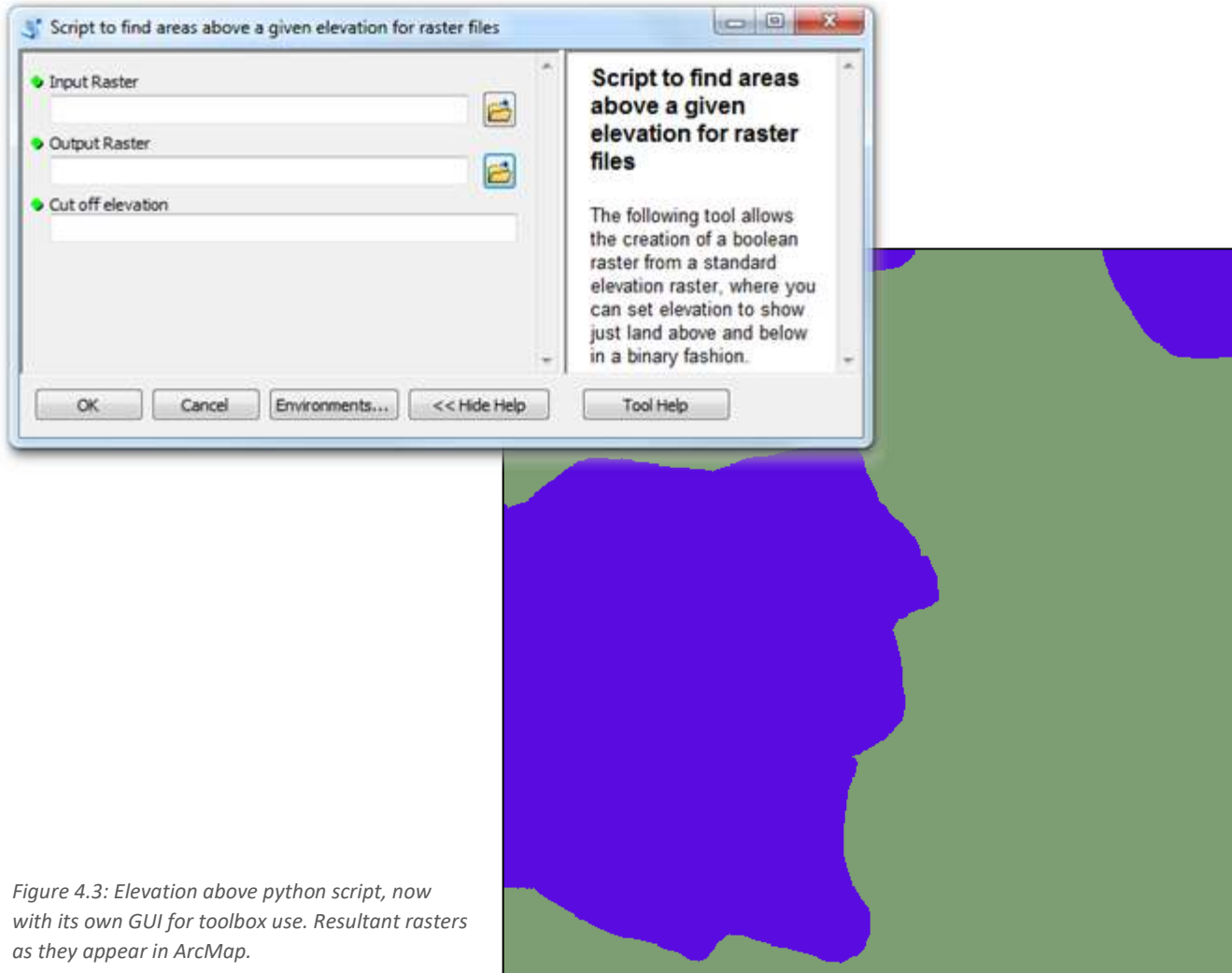


Figure 4.3: Elevation above python script, now with its own GUI for toolbox use. Resultant rasters as they appear in ArcMap.

4.3 Batch processing python script

While the above takes a single raster it is required often to repeat this process over many files, below is code used when creating the batch script.

```
1. '''This script uses map algebra to find values in an elevation raster greater than a specified value.'''
2. import os
3. import arcpy
4. #switches on Spatial Analyst
5. arcpy.CheckOutExtension('Spatial')
6. #loads the spatial analyst module
7. from arcpy.sa import *
8. #overwrites any previous files of same name
9. arcpy.overwriteOutput=True
10. #Specify the input folder and cut-offs
11. inDirectory = arcpy.GetParameterAsText(0)
12. cutoffElevation = int(arcpy.GetParameterAsText(1) )
13. #Process the .img files in the directory
14. for i in os.listdir(inDirectory):
15.     if os.path.splitext(i)[1] == '.img':
16.         inRaster = os.path.join(inDirectory, i)
17.         outRaster = os.path.join(inDirectory, os.path.splitext(i)[0] + '_above_' + str(cutoffElevation) + '.img')
18.         #Make a map algebra expression and save the resulting raster
19.         tmpRaster = Raster(inRaster) > cutoffElevation
20.         tmpRaster.save(outRaster)
21. #Switch off Spatial Analyst
22. arcpy.CheckInExtension('Spatial')
```

Figure 4.4: Boolean raster creation for a batch of files allowing for specific elevation value (python code), with green descriptors for how each line functions.

Below is the resultant raster and script GUI with including classification method for GUI.

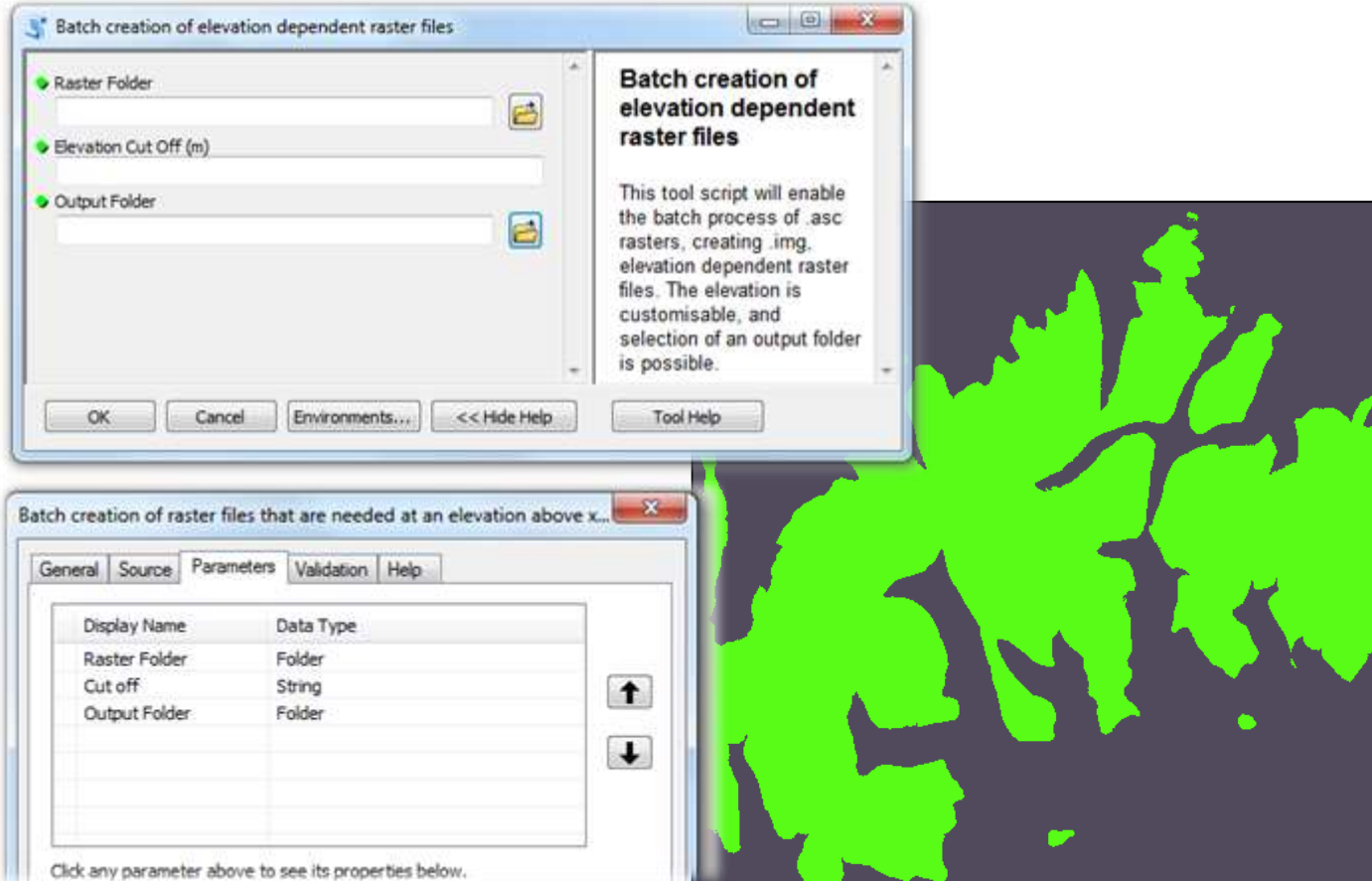


Figure 4.5: Boolean raster creation for a batch of files allowing for specific elevation value, now with its own GUI for toolbox use. Resultant rasters as they appear in ArcMap.

4.4 Complex operations: Brown Trousers

Following the creation of previous tools in tasks above, the final result was to combine them to automate the workflow from section 3.0 ‘Multi-Criteria Analysis’. Here is evidence of the time saving python can offer and the end result, along with the tools GUI.

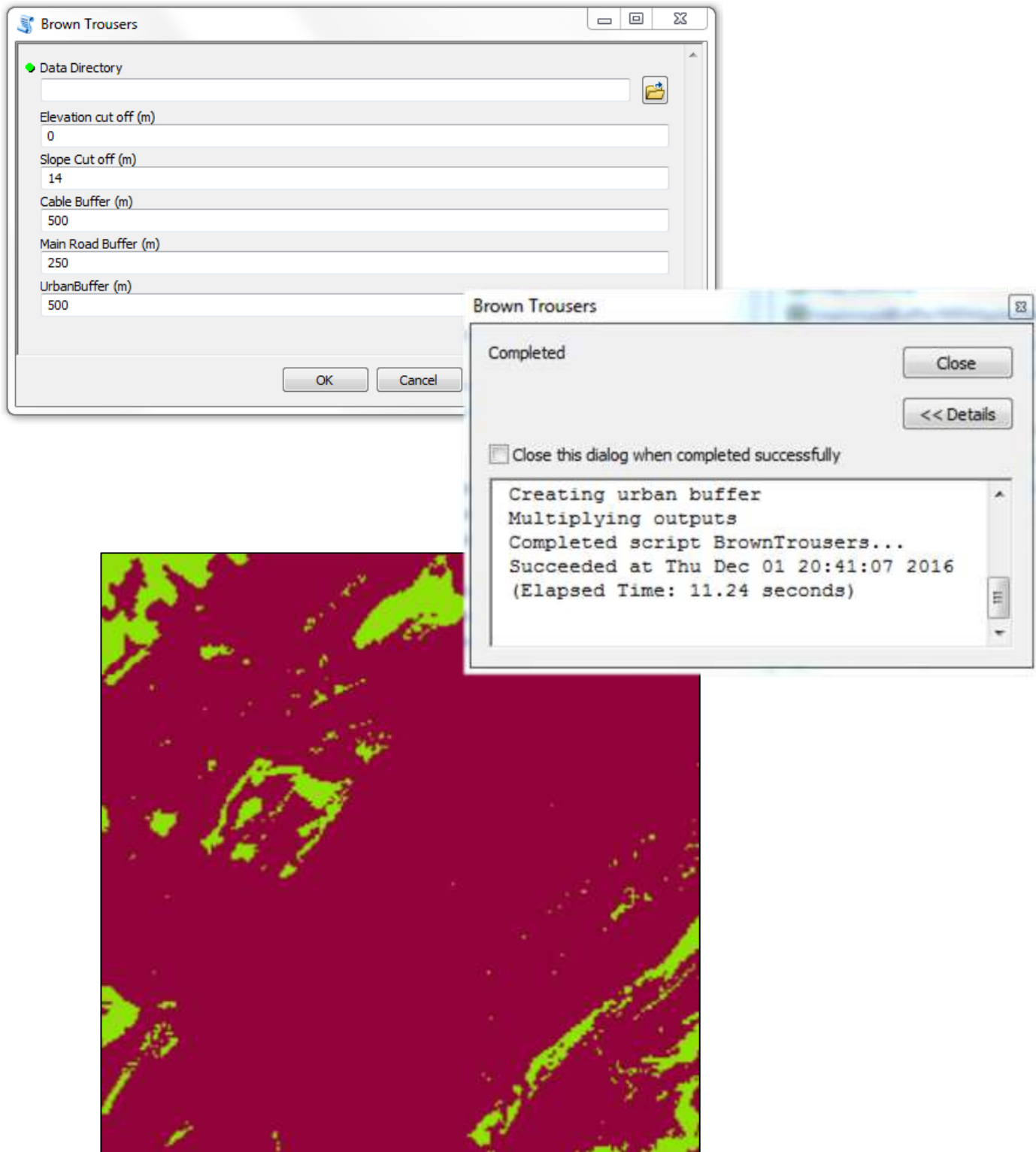


Figure 4.6: Images showing complex processing GUI, with its resultant raster and how quickly it created this layer: 11.24 seconds.

5.0 Assessing land cover change: Mato Grosso, Brazil

5.1 Introduction

The Amazon rainforest has been an area of large debate, media attention and environmental importance. Mato Grosso state in Brazil – part of the amazon rainforest – is a threshold location for land use change over a relatively small time period.

5.1.1 Vegetation clearance in Mato Grosso, Brazil

Deforestation is a timeless issue for mankind, Middleton (2008) discusses how often deforestation was a method used for development between eras, from hunter gatherer to more sustainable farming for a civilization, however today it is fair to say things have got out of hand. Deforestation has shown exponential growth within the Amazon rainforest, as illustrated by Fearnside (1982). The Detrimental effects of deforestation can be seen globally from climate change to soil degradation. While areas of the northern hemisphere are moving towards more sustainable agricultural practices, the areas of the tropics have been deforesting at a rate of 14.m ha a year, between 1990 and 2000 (FAO, 2001). Middleton (2008) also addresses how “national government is another factor in encouraging certain groups to use the forest resource” this factor coupled with mobility and access to widespread rainforest in brazil, accounts for deforestation on such a large scale.

5.1.2 Remote sensing: Tool for land cover change analysis

Satellite imagery has become the most effective way of viewing the surface of our planet. It enables the viewing of extended parts of earth at the click of a button. Due to the easy access of data through places such as the USGS, up to date studies are possible and frequent analysis can be performed meaning mitigation is at the forefront of research. Landsat data is one of the most accessible and in 1997/98 data from Landsat was able to determine levels of Amazonian deforestation and by measure hectare loss per year could learn about the size of the culprits, often being medium to large landowners and not the often blamed small landowners (Indiana University, 2007).

5.2 Study Topic and Methodology

5.2.1 Mato Grosso

Mato Grosso is one of the 26 states of Brazil, and is dominated primarily by rainforest. Modern day Mato Grosso has a large agricultural sector, namely the export of soybean (Brazil.org.za, 2016). The area of study in focus is marginal land between dense forest and agricultural development, the assessment will consider one image from 1990 and another from 2005.



5.2.2 Data Source

The two satellite images assessed were from 1990 and 2005 and both collected using Landsat satellites. Landsat 5 TM captured the 1990 image on the 3rd July, while Landsat 7 ETM+ captured the 2005 image on the 14th July. This

imagery was then downloaded for use from the Global Landcover Facility website. Pixel resolution was 30 metres x 30 metres. The projection was WGS 84 and from zone 21, UTM.

5.2.3 Analysis Method

Initial analysis was carried out upon two original image files, these images were captured by Landsat thematic mapper sensor which captures seven bands of data (Gibson & Power, 2000), one of which being Near Infra-Red or NIR. The images used were NIR based images which enabled further analysis of Normalised Difference Vegetation Index (NDVI), Image Difference and lastly unsupervised classification thematic mapping.

5.2.3.1 Normalised Difference Vegetation Index

This form of analysis forms an image derived from reflectance and vegetation cover characteristics.

$$NDVI = \frac{(NIR - RED)}{(NIR + RED)}$$

Figure 2: Normalised Difference Vegetation Index Formula

The black and white image formed reduces the colours used to just black and white, where white represents vegetation and black represents bare ground. NDVI classes the pixels of the continuous data image file from -1 to +1, with negative values being water, values near zero being clear ground and positive values ranging from sparse vegetation to dense forest. Figure 3 is an example of the basic results from this analysis.

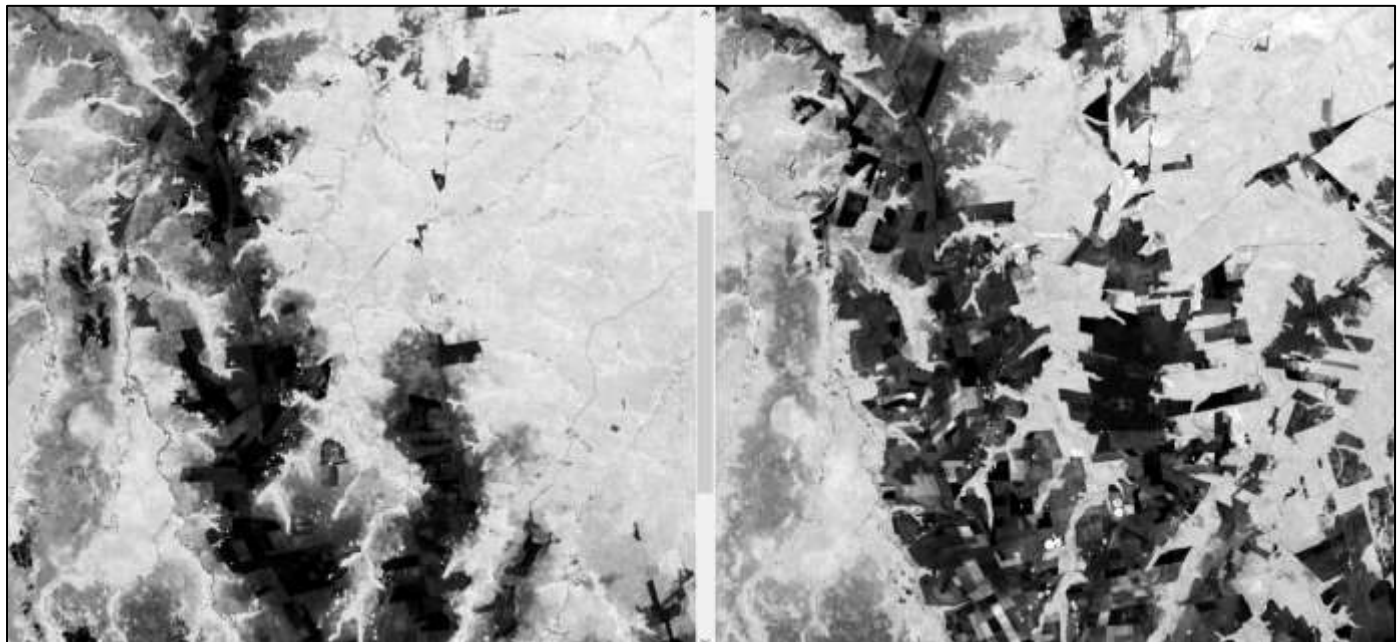


Figure 3: Image showing 1990 (left) NDVI close up comparison to 2005 (right) NDVI close up result.

5.2.3.2 Image Difference and Highlight Change

With the creation of two NDVI images for 1990 and 2005 it became necessary to accurately view change between them. Image difference analysis enables automated assessment of difference between two images. The image difference file is a subtraction of the initial 1990 data from the 2005 data, whereas highlight change shows percentage change banded into differing colours, red through to green.

I chose increment changes of 0.5% for highlight change as it removed most of the background unclassified change and sorted it within the relevant change categories as managed from the attribute table.

5.2.3.3 Unsupervised Classification: Thematic Mapping

This area of analysis enabled land use mapping with a focus on land use change between 1990 and 2005. The controlling variable on file outcome here was class number when performing the classification, after trying many different amounts, I found 12 to give the most efficient amount of differentiation while not being too picky so that the final classes were poorly split. The process is shown in figure 4.

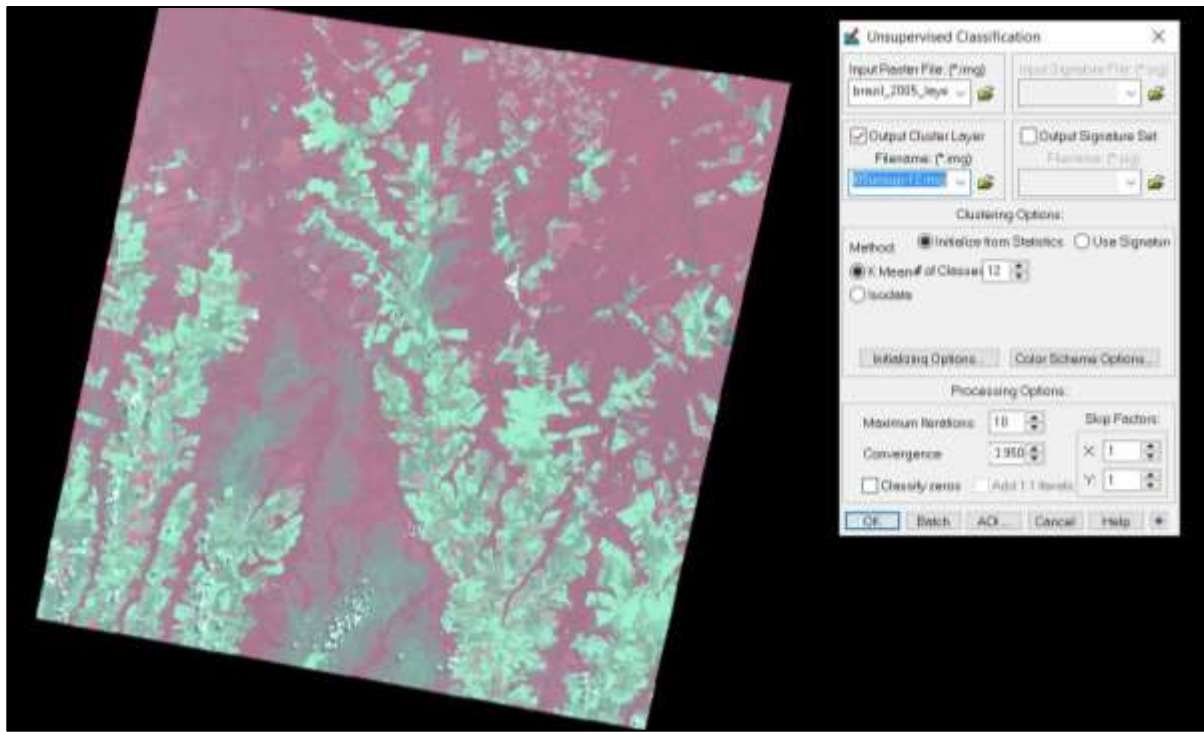


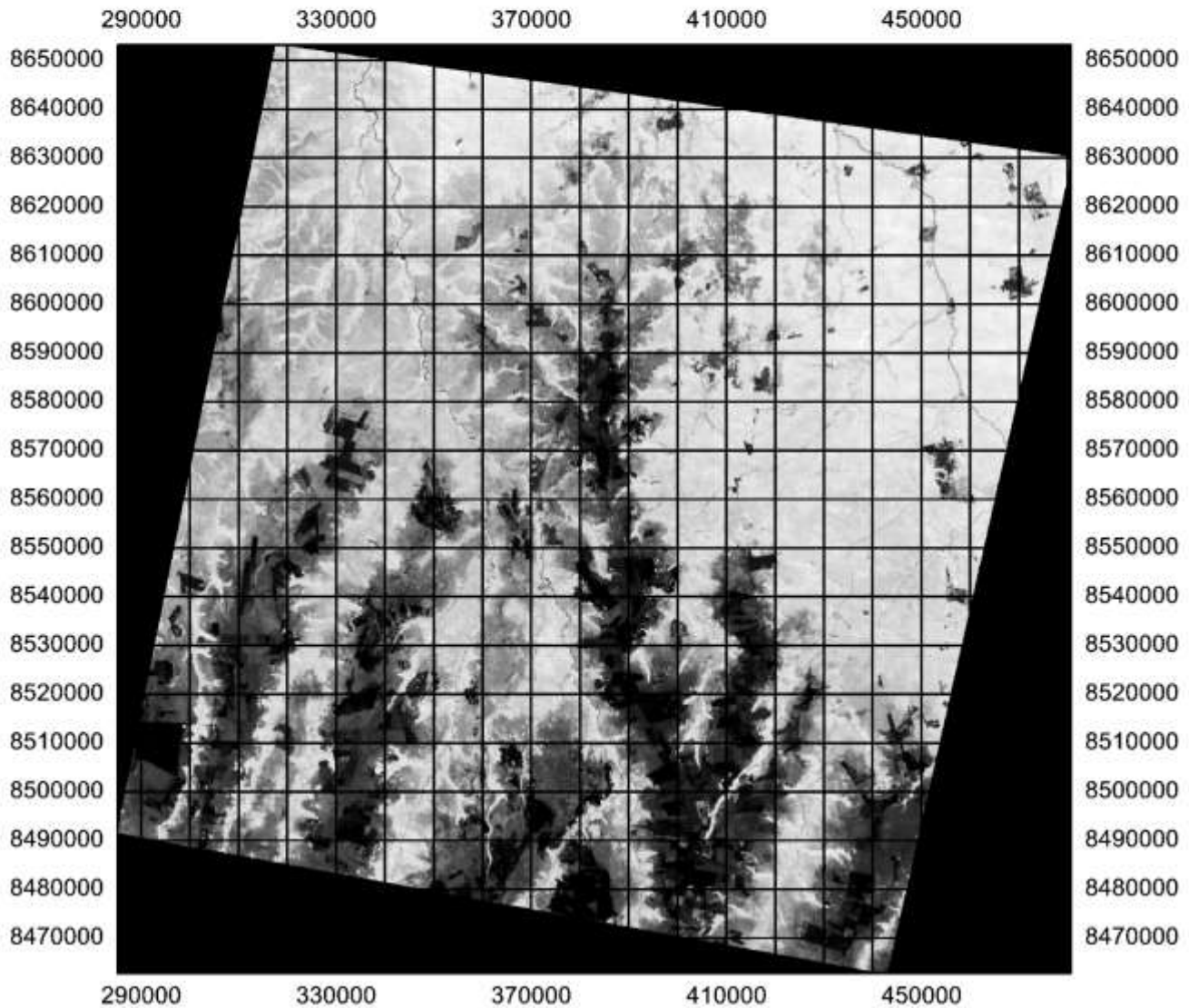
Figure 4: Image showing 2005 image undergoing unsupervised classification using a class size of 12. Source: ERDAS Imagine.

Lastly the image split into resulting classes was merged into 5 to 6 classes and recoloured to give the best image outcome.

Mato Grosso 1990 Vegetation Map

NDVI Analysis

Full extent



1 : 1237050.31



Scale

5000 0 5000 km

1 : 181779918.64

Figure 5: NDVI Analysis map of 1990 Mato Grosso, Brazil.

Mato Grosso 1990 Vegetation Map

NDVI Analysis

Close up extent

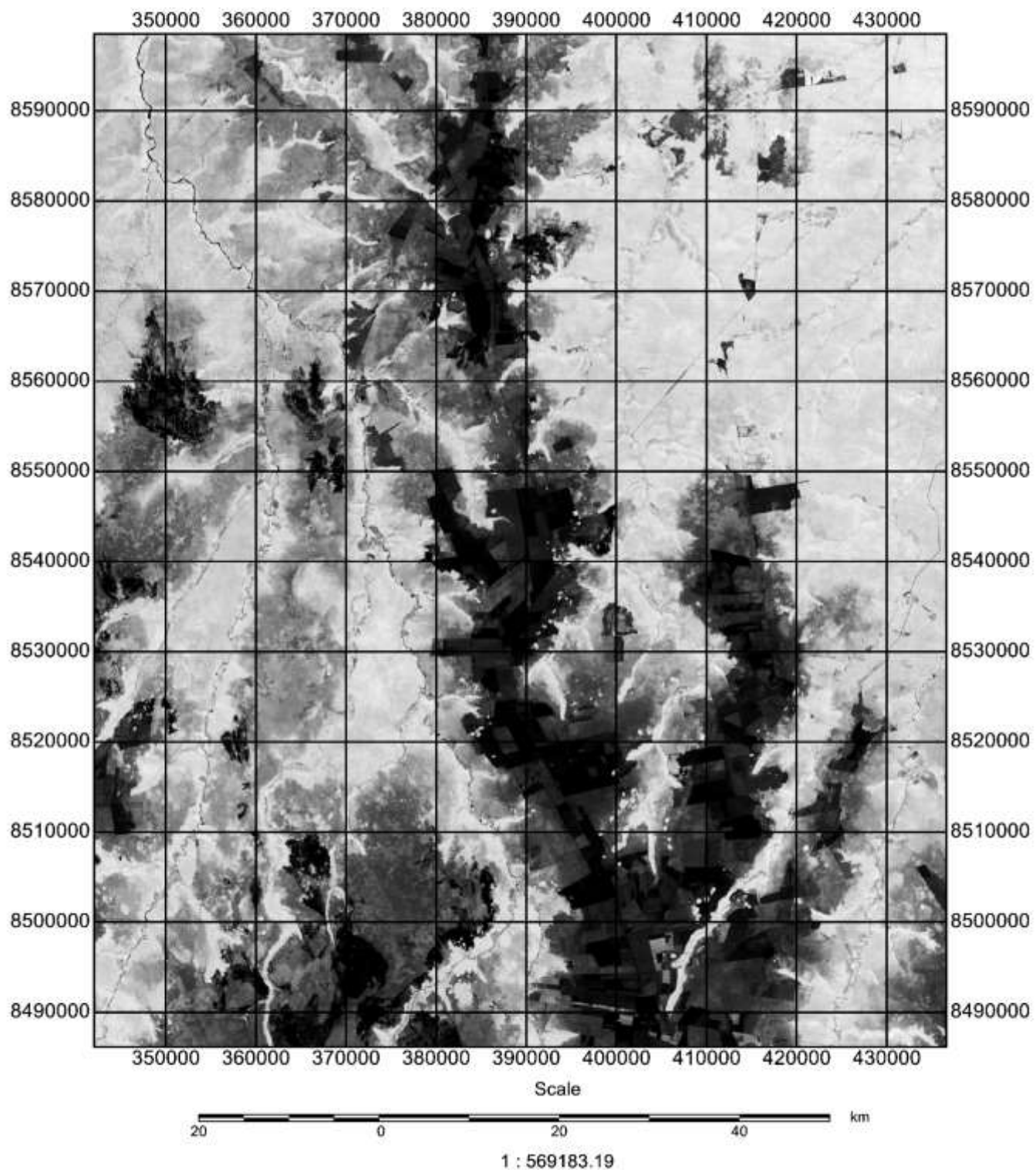
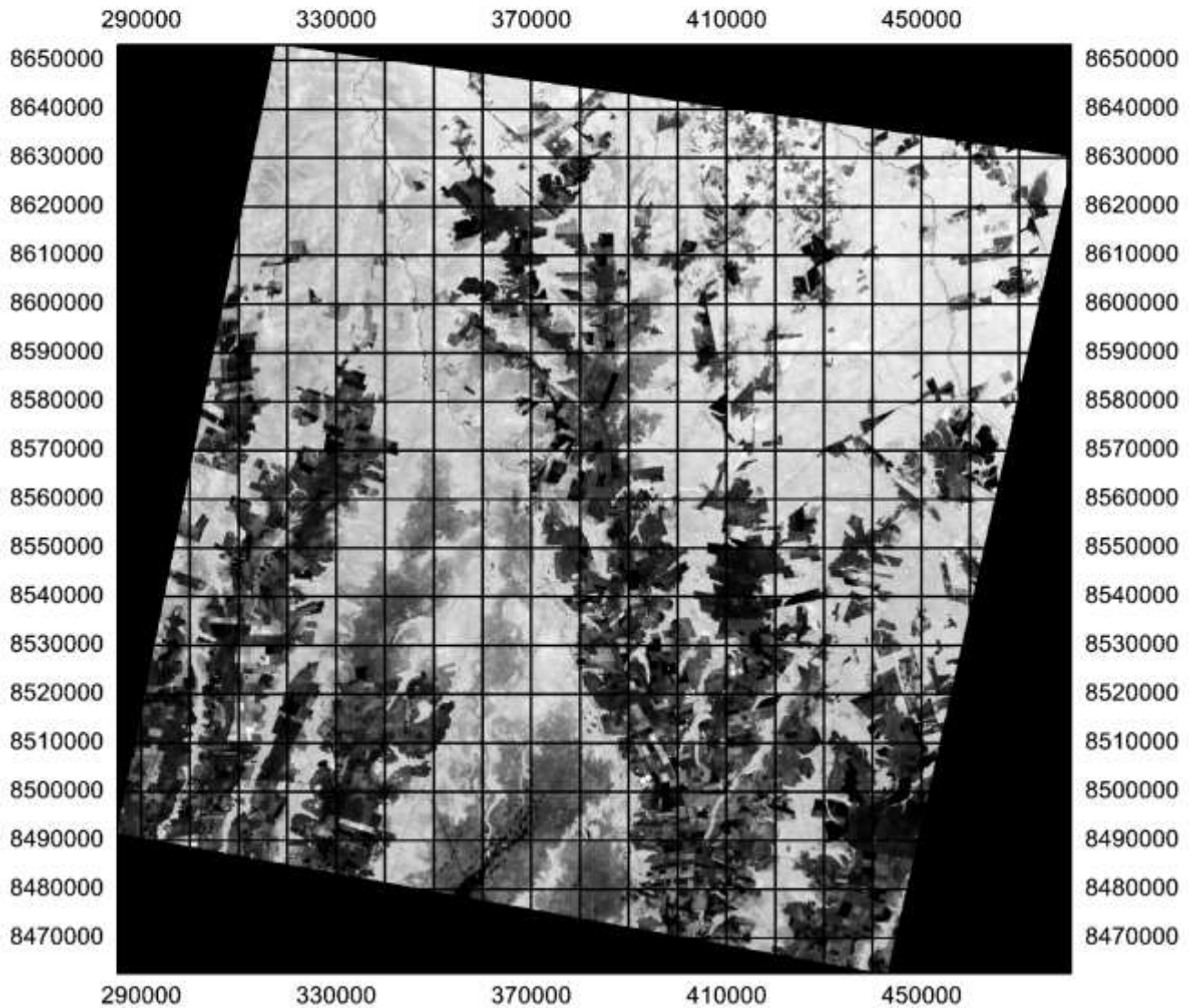


Figure 6: NDVI Analysis map of 1990 Mato Grosso, Brazil. Close up extent.

Mato Grosso 2005 Vegetation Map

NDVI Analysis

Full extent



Scale



1 : 1237050.31



Scale



1 : 181779918.64

Figure 7: NDVI Analysis map of 2005 Mato Grosso, Brazil.

Mato Grosso 2005 Vegetation Map

NDVI Analysis

Close up extent

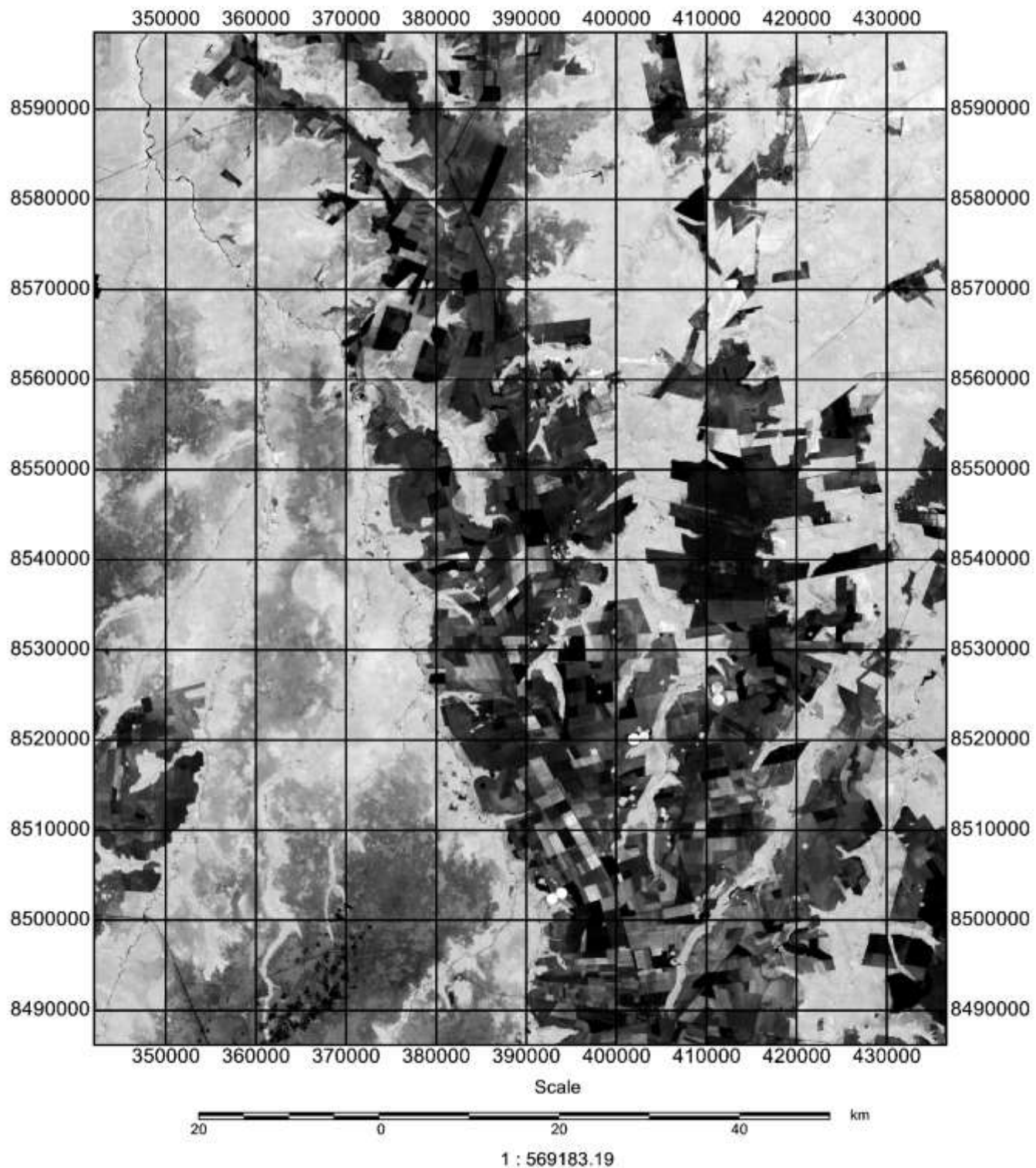
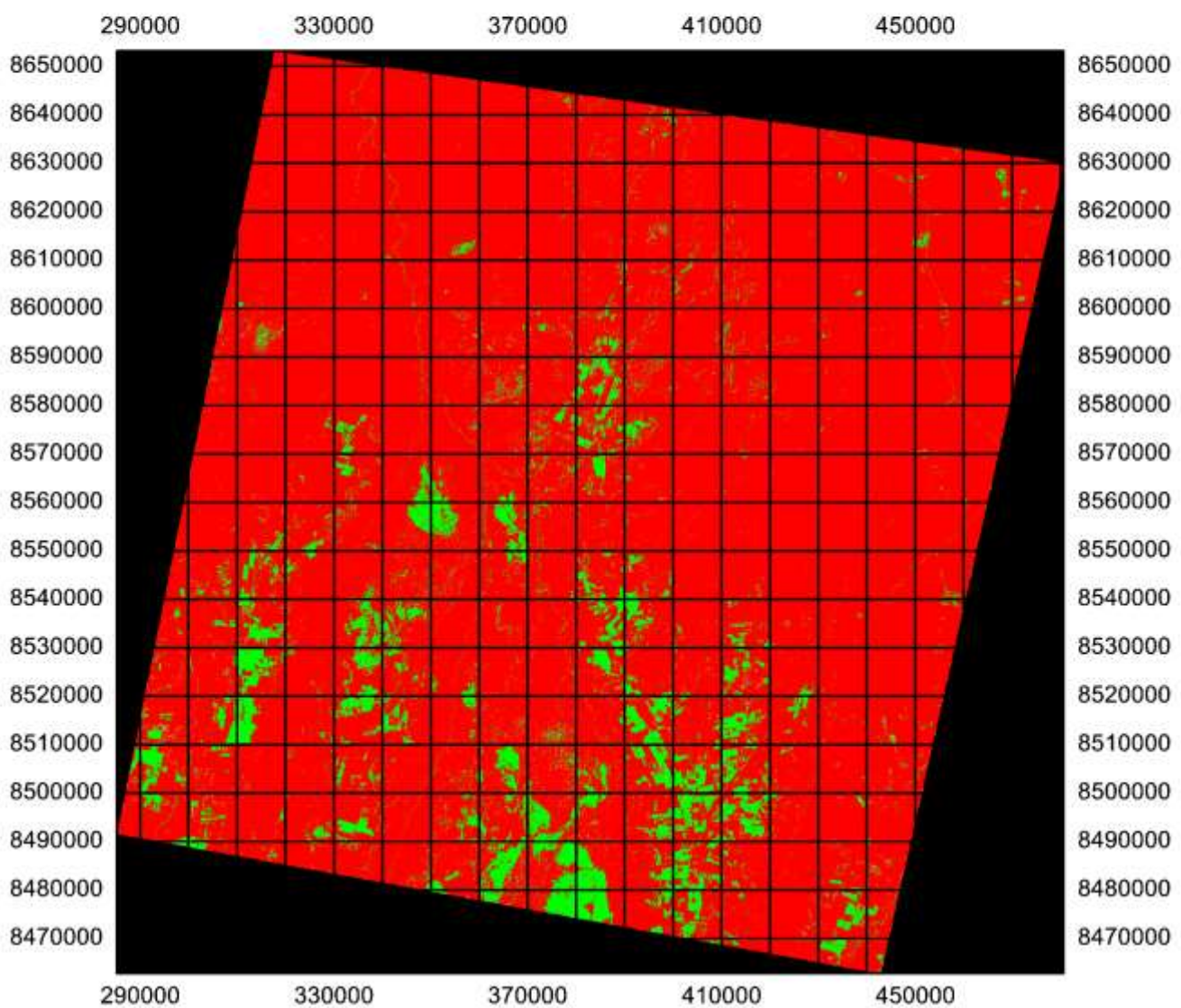


Figure 8: NDVI Analysis map of 2005 Mato Grosso, Brazil. Close up extent.

Mato Grosso 1990 - 2005 Vegetation Map

Highlight Change

Full extent



1 : 1237050.31

Vegetation Change

- █ Decreased
- █ Some Decrease
- █ Unchanged
- █ Some Increase
- █ Increased



Scale

5000 0 5000 km

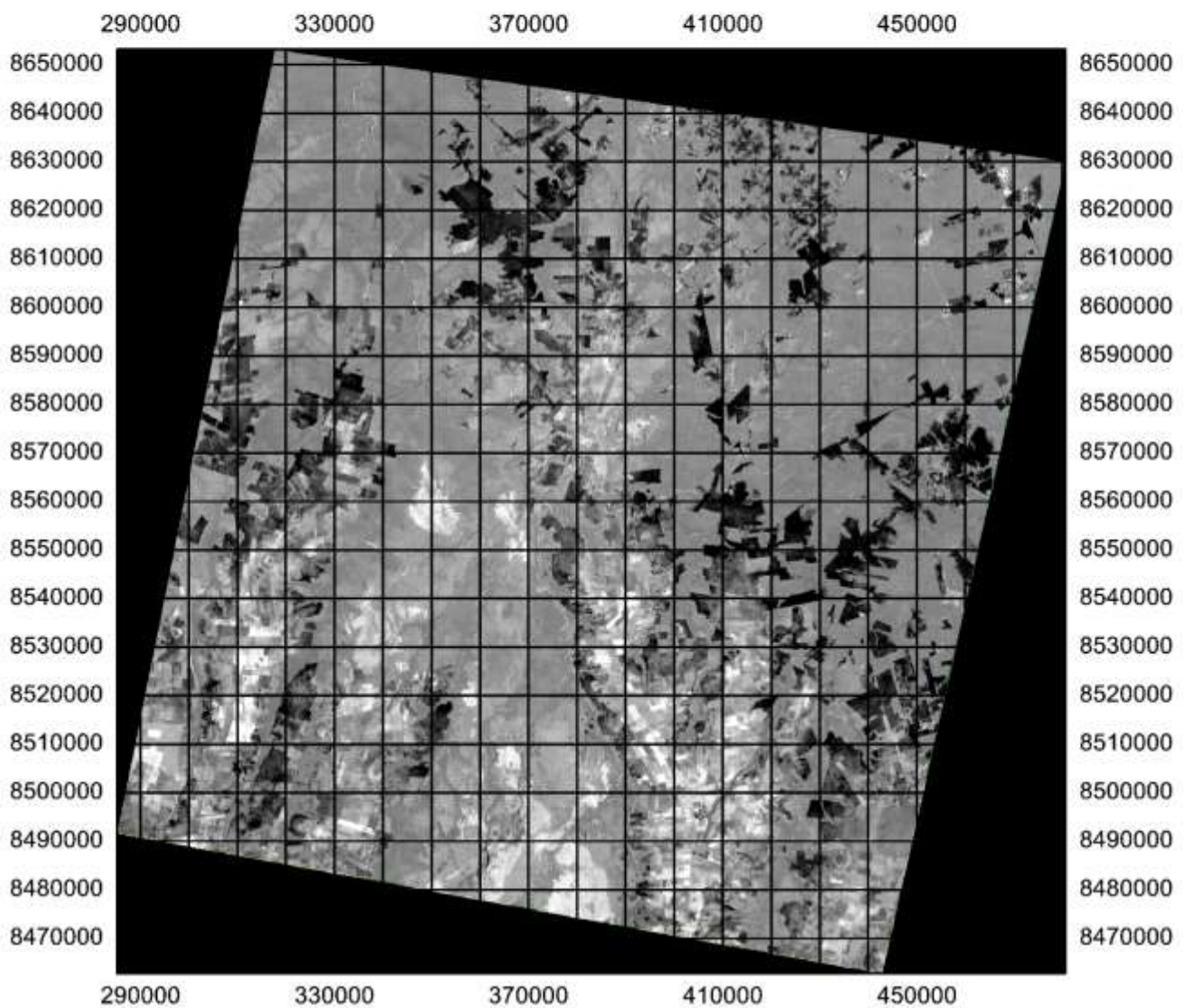
1 : 181779918.64

Figure 9: Highlight change map of Mato Grosso, Brazil. Showing vegetation decrease (red) to increase (green) between 1990 and 2005.

Mato Grosso 1990 - 2005 Vegetation Map

Image Difference

Full extent



Scale



1 : 1237050.31



Scale



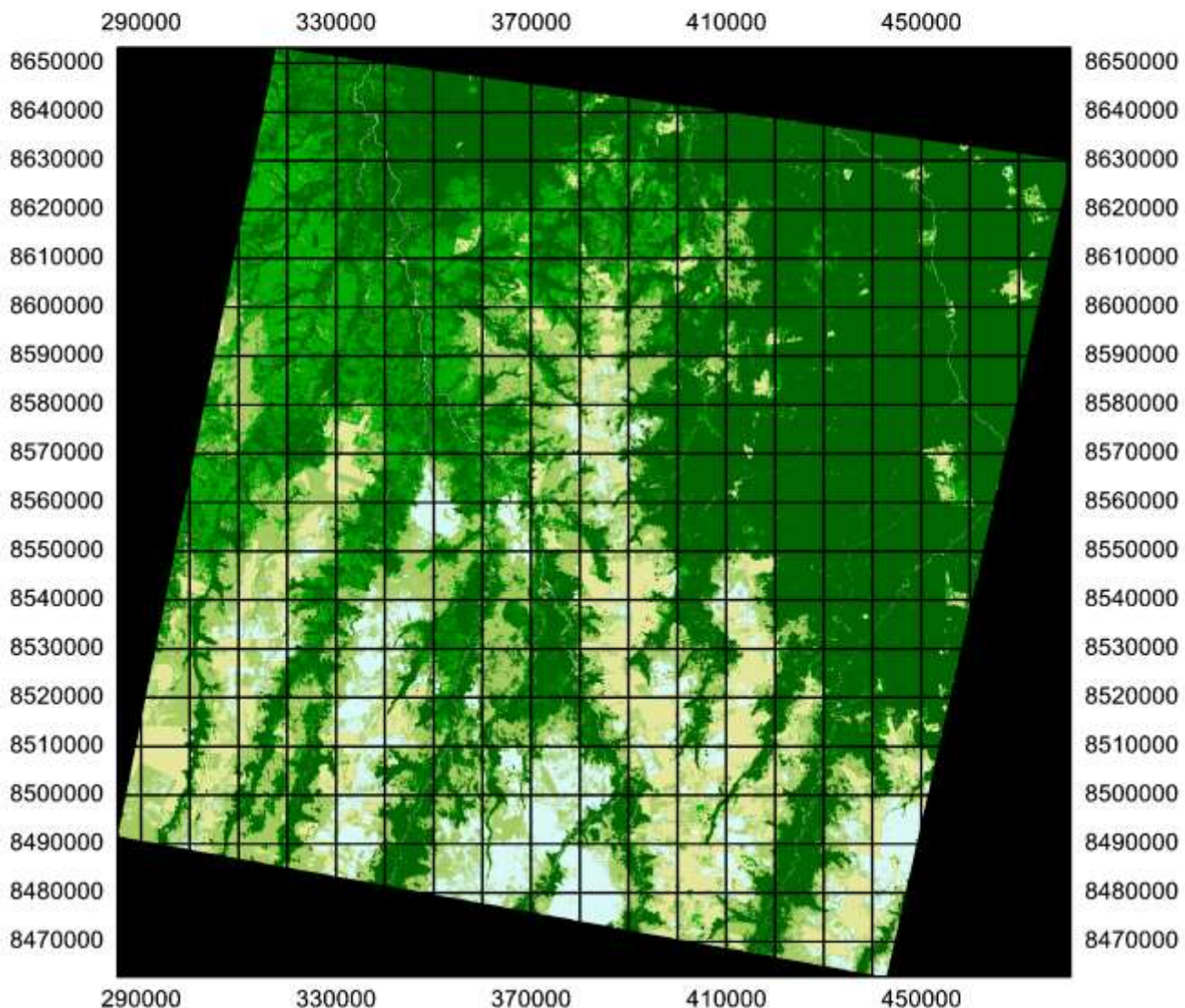
1 : 181779918.64

Figure 10: Image difference map of Mato Grosso, Brazil. Showing direct change in vegetation between 1990 and 2005.

Mato Grosso 1990 Vegetation Map

Land Cover Change

Full extent



Scale
50 0 50 100 km
1 : 1237050.31

Land Use Type	
Dense Forest	
Marginal Forest	
Bare Land	
Agricultural Land	
Water	



Scale
5000 0 5000 km
1 : 181779918.64

Figure 11: Land cover change map of 1990 Mato Grosso, Brazil.

Mato Grosso 1990 Vegetation Map

Land Cover Change

Close up extent

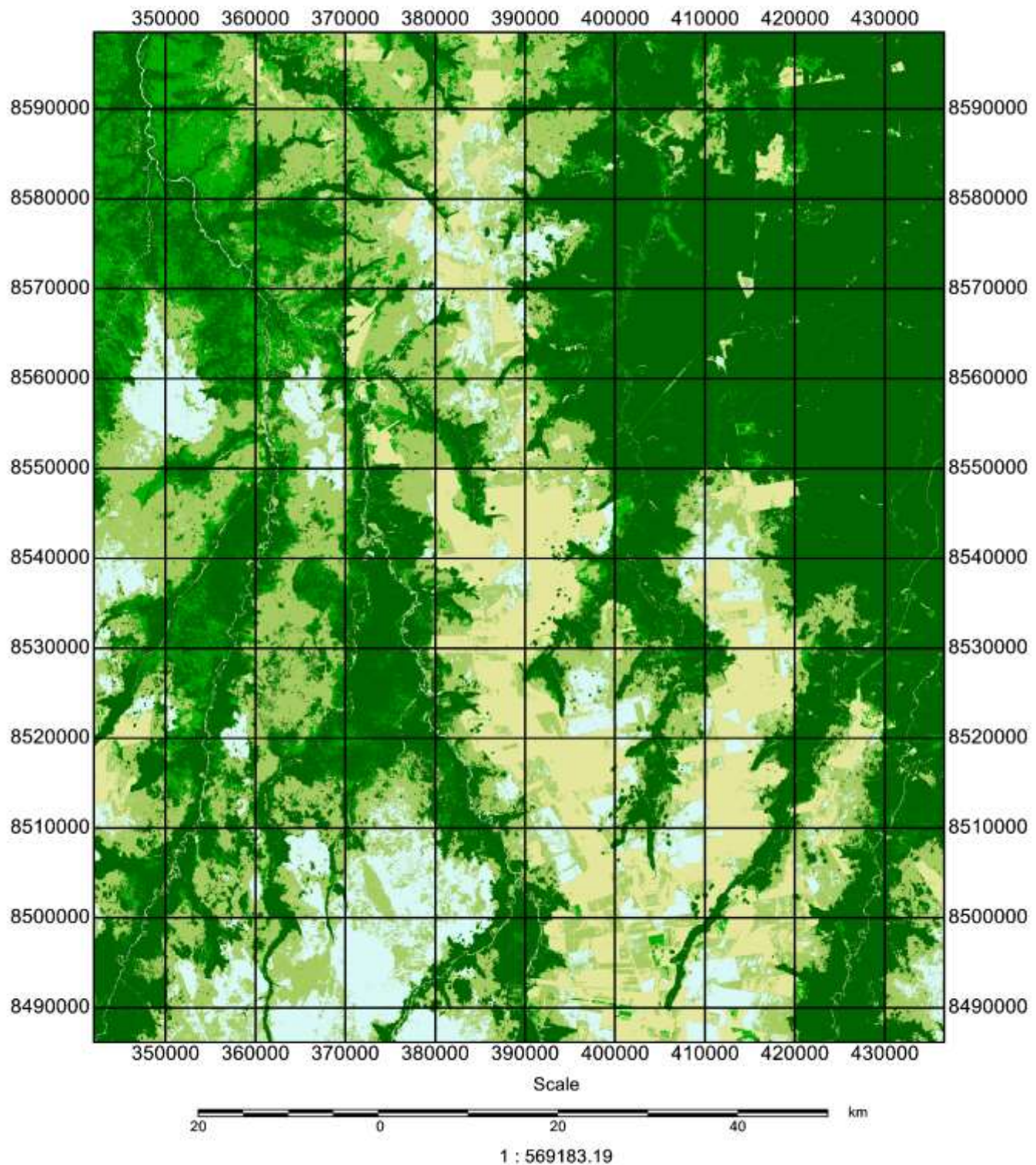
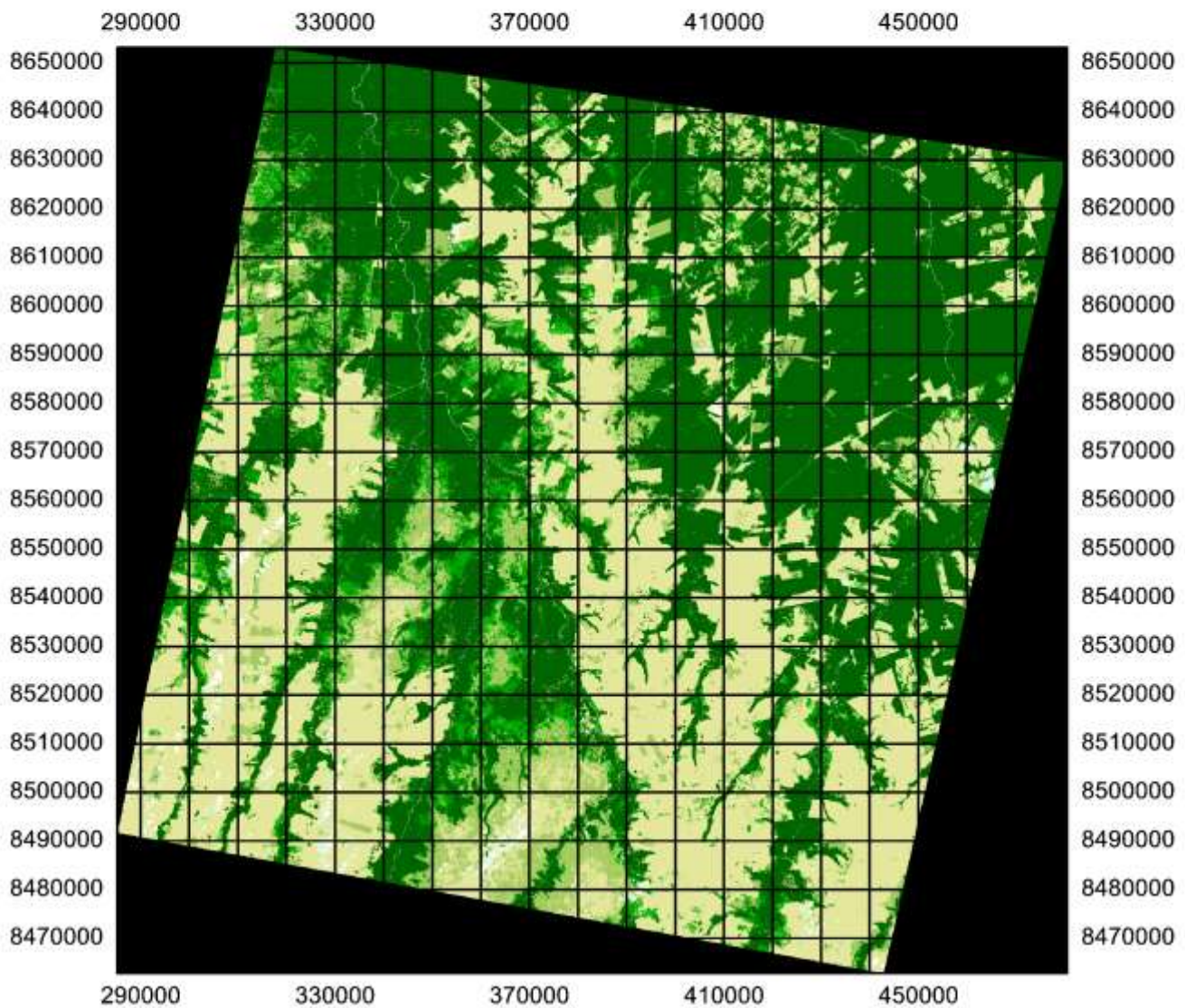


Figure 12: Land cover change map of 1990 Mato Grosso, Brazil. Close up extent.

Mato Grosso 2005 Vegetation Map

Land Cover Change

Full extent



Scale



1 : 1237050.31

Land Use Type

- [Dark Green] Dense Forest
- [Medium Green] Marginal Forest
- [Light Green] Bare Land
- [Yellow] Agricultural Land
- [White] Cloud
- [Light Blue] Water



Scale



1 : 181779918.64

Figure 13: Land cover change map of 2005 Mato Grosso, Brazil.

Mato Grosso 2005 Vegetation Map

Land Cover Change

Close up extent

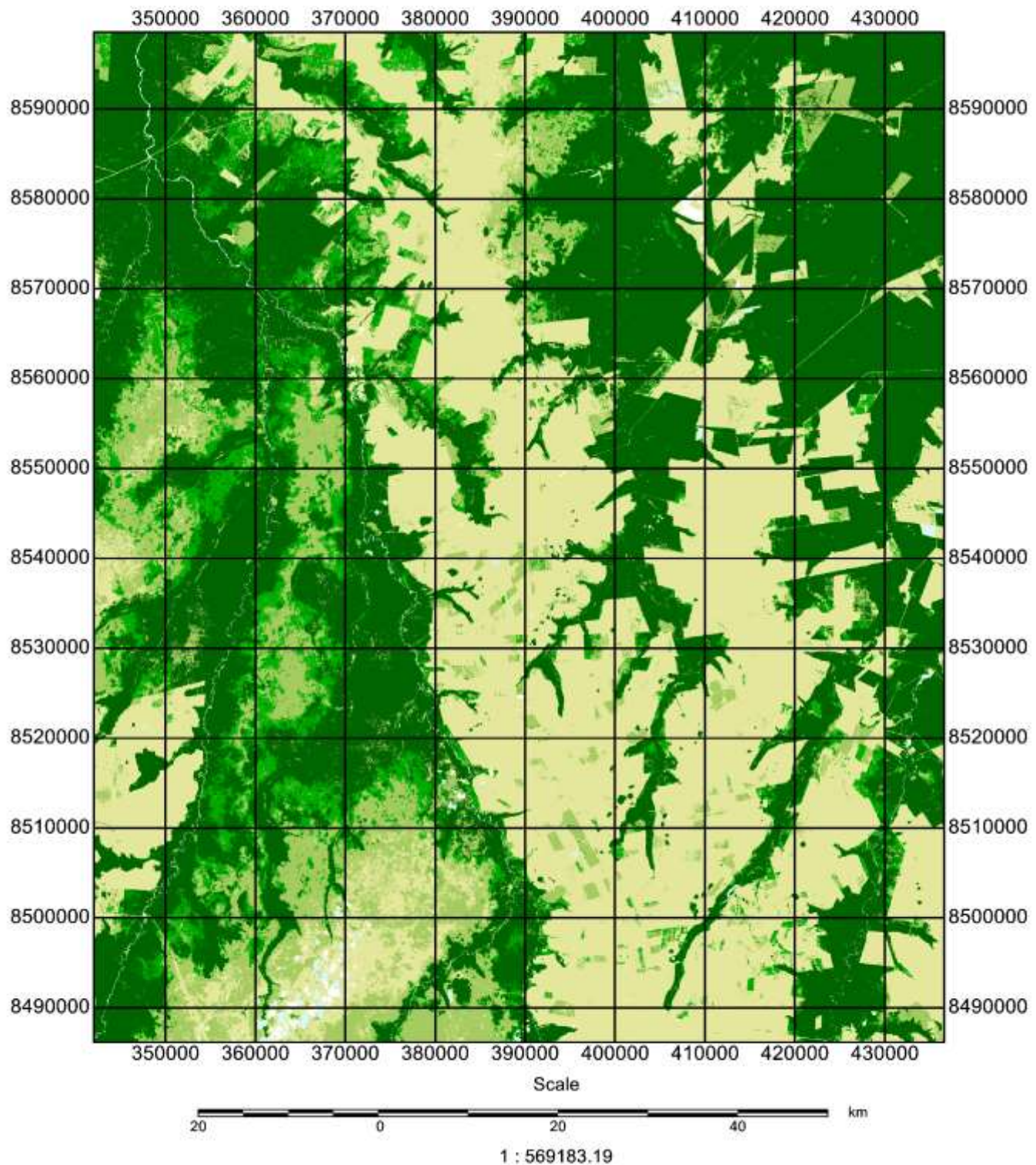


Figure 14: Land cover change map of 2005 Mato Grosso, Brazil. Close up extent.

5.3 Results

5.3.1 NDVI

Initially the NDVI Results show a clear change in vegetation land cover, from forested land to increased bare ground. Figure 5 and 7 highlight the change that has occurred over the whole research area, there has been a sprawling growth from what was once there in 1990 outwards into the forest by 2005, this is represented by the increased black ground (bare ground). Figure 6 and 8 where a closer view of the where the change has occurred. There has also been new bare ground growth in 2005 that has not grown from previous bare ground but been created in the middle of forested area.

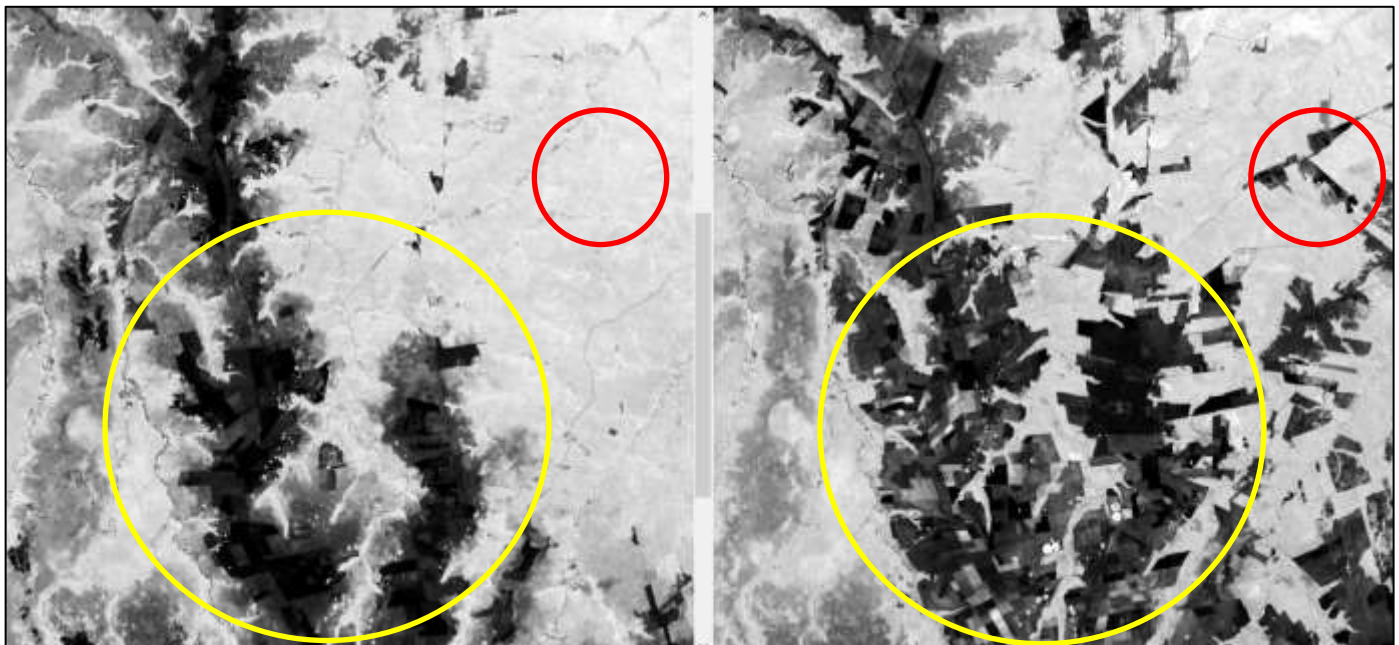


Figure 15: NDVI close up view highlighting areas of particular change between 1990 and 2005 in Mato Grosso, Brazil.

The yellow circles above in figure 15 highlights sprawling growth of bare ground, whereas the red circles represent new creation of bare ground.

5.3.2 Highlight Change

Highlight change shows important results, as is evident from figure 9 there is a dramatic amount of decrease in vegetation between the two pictures, the NDVI hints at this change but struggles to so the severity compared to highlight change. There is small amounts increase but this is generally marginal agriculture/forest or high ground. The red increase is obvious and seems to match increased bare ground from the NDVI and show a general deforestation across the whole area.

5.3.3 Land Cover Change – Thematic Maps

Here we able to combine the quantified highlight change and the NDVI to give a layer-by-layer view of differing land cover and its change over time. Figures 11 and 13 show the full extent while 12 and 14 show a close up comparison. These maps are able to categorise land cover and show growth and reduction.

Land Cover	Area (Hectares)		Percentage		Land cover change between 1990 - 2005 (Percentage)
	1990	2005	1990	2005	
Dense Forest	1400000	1261700	51.30%	46.29%	-10%
Marginal Forest	353137	189620	12.94%	6.96%	-46%
Bare Land	530742	294536	19.45%	10.81%	-45%
Agricultural Land	238819	947695	8.75%	34.77%	297%
Water	206544	18387.5	7.57%	0.67%	91%
Clouds	0	13729	0.00%	0.50%	N/A

Table 1: Table showing area change from the Highlight Change analysis of Mato Grosso, Brazil.

Table 1 above quantifies the change from figures 12 and 13, with a increase of 297% agricultural coverage between the dates that accounts for the vast change in beige shown on the thematic maps, however they also show an increased level of development from residents/workers of the area, -45% bare land shows the ability to turn bare land into arable land.

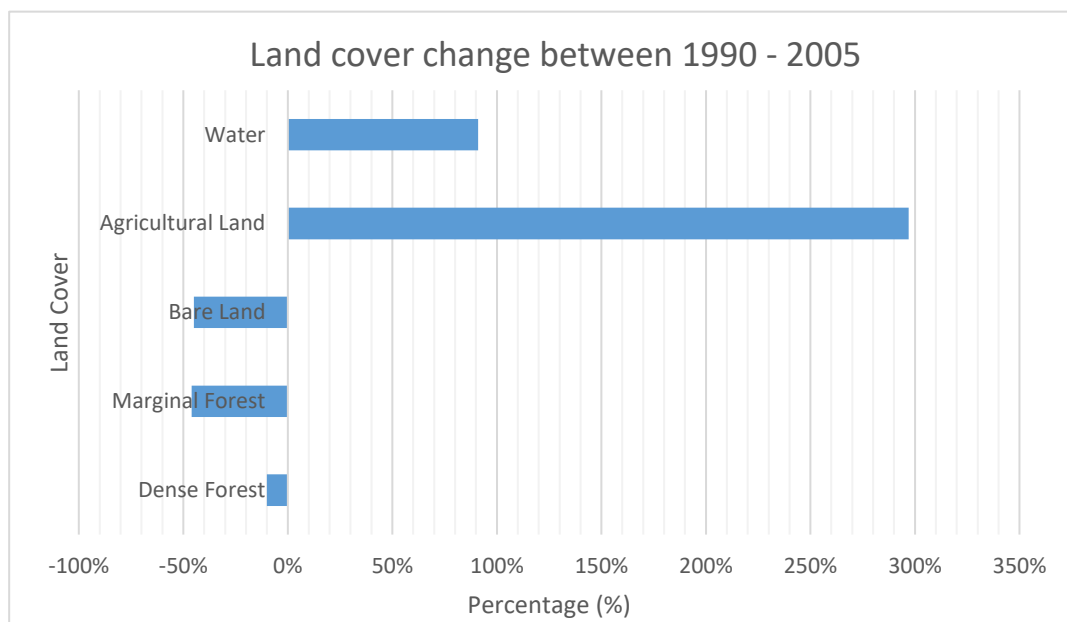


Figure 16: Graph showing percentage land cover change between 1990 and 2005 of Mato Grosso, Brazil.

One anomalous result is the increase in water shown in figure 16, however findings showed that cloud shadow – which is more apparent on figure 13 (2005) – matched a similar class colour as bare water and therefore this may account for the dramatic increase in water.

5.4 Discussion

The increased deforestation and subsequent vegetation loss can be explained by two factors one being an industry wide agriculture crop change and another being area development.

Since the 1970s citizens were encouraged to clear Amazonian forest to expand cropped area to rear cattle (Arvor et al, 2012), however this steady expansion does not reflect the data seen from the analysis of maps above. Mato Grosso over the 15 years assessed here has undergone rapid expansion, from widespread cattle farming to industrialised soybean production, in 2012 soybean provided for 31.3% of its national produce (Arvor et al, 2012) and it was expected that “each square kilometre of soybean production supports 2.5 formal sector jobs” (Richards et al, 2015). Due to the booming industry, the amazon forest has suffered with clearance of forest and cerrado to make way for a growth of 13.6 to 23.4 million hectares soybean cropland from 2000 to 2005 (Richards et al, 2015). This expansion of industry accounts for the initial changing NDVI and later the severe thematic map change of +297% agricultural land over just 15 years.

It is expected that new licencing and control of clearing will decrease deforestation across Mato Grosso according to Fearnside (2003). However this doesn't seem to be a permanent, as recently as November 2015 The Guardian released an article stating a rise of 16% deforestation (Wicks, 2015), there is still a long way to go.

5.4.1 Limitation

Cloud cover caused issue when it came to classification, often it layered within the water layer and therefore gave inaccurate data as seen in table 1. Also with cloud covering land it actually resulted in missing data. After more research it is possible to nullify the cloud effect by editing your raster layer in ArcMap, digitizing your clouds and revaluing them (Ce.utexas.edu, 2016) with more time this could be done.

5.5 Conclusion

The analysis of Mato Grosso's growing deforestation and vegetation loss highlighted important factors within the use of satellite imagery as a means of assessing areas land cover change and links to social, economic motives. In the case of Brazil, Mato Grosso is providing a healthy revenue for countrywide development, from new found soybean farming and as a result, regulations upon deforestation are slack. The NDVI analysis of figure 5 and 7, and the thematic map analysis of figure 11 and 13, as well as highlight change provide evidence for the severity of the over production and impact upon the Amazon. With agriculture rising by 297% and dense and marginal forests reducing by a combined -56%, it is hard to see any change to this practice without an environmental focused intervention.

6.0 Land Surveying of Portland Building, Portsmouth.

The aim of this practical was to perform an extensive survey of Portland Building, University of Portsmouth, Portsmouth. This was carried out using a prism and the Topcon OS-103 total station with a device accuracy of down to 3 inches (Topcon OS Series, 2013) to assess the area of the quadrangle and Portland building. Initially a set of control points and their corresponding co-ordinates were given, the points in the diagram below illustrate the control points, while the table shows the information for each point.



CP No.	Easting	Northing	Elevation
1	463629.428	100222.711	3.031
2	463602.444	100223.879	2.717
3	463532.576	100247.673	2.862
4	463551.467	100309.206	3.337
5	463604.398	100249.328	2.724

Figure 1: Illustration of Portland control points, including a table representing their corresponding easting, northing and elevation.

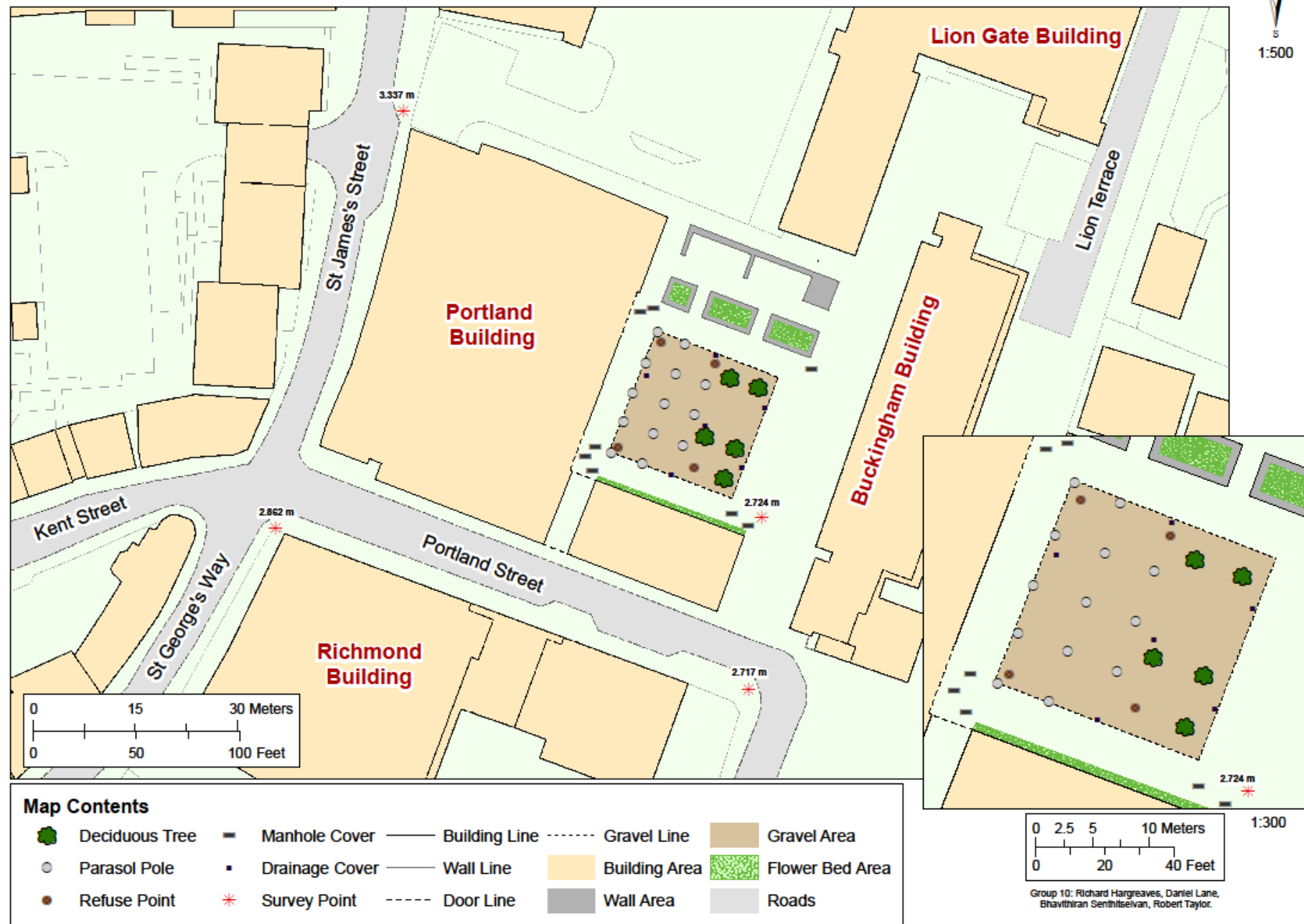
Calibration of the total station was then performed above control point 5 for the internal Portland survey, including the quadrangle. The external survey required calibration of points 2, 3 and 4. Calibration involved, levelling and positioning of the station upon its tripod above a ground marker. This was done using the manual level circle on the total station and once within the manual margins it was precisely levelled using the electronic leveller within the device. Lastly a back sight was taken to another known control point, for example a back sight to point 2 from point 5. This back sight enabled the total station to know its location in space. Once a place in space was established the survey could now be undertaken.

The survey is performed with the prism and the station, the surveyor would position themselves upon a point they wish to survey with the prism

being held vertical, as decided using the manual leveller. Then the total station would be adjusted so that the prism was in line of sight, and with a click of button the point was surveyed. There was initial preparation required within the menus, depending on the point being surveyed it was useful to choose differing codes, for example if a point on a wall was surveyed, the station would be programmed to record it as a wall line point, and if a manhole cover was being surveyed it would be recorded as a man hole cover. The code was changed depending on what the surveyor decided was appropriate for the task at hand. Once the area had been surveyed the point and line data was transferred to a USB ready for processing within ArcMap.

The results collected comprised of a range of classified survey points that were later processed within ArcMap to create a variety of point and polygon features. Processing included classification of points and joining of lines/points to form whole polygons, the process: ArcToolbox – Data Management Tools – Features – Feature to Polygon, was then used to create polygon layers which allowed building and area classification. The relevant classes and colours decided formed the main information layer of the map. Also zoomed data frames can be useful when viewing detailed areas at a smaller scale to enable easier measurement of distances, this technique was applied to the quadrangle, to clearly show position and distances between the clustered features. Lastly the addition of a north arrow, legend, scale bar and title completed the final map

Portland Building and the Quadrangle, North Quarter, University of Portsmouth



7.0 Bibliography

7.1 Literature:

- Arvor, D., Meirelles, M., Dubreuil, V., BÃ©guÃ©, A., & Shimabukuro, Y. (2012). Analyzing the agricultural transition in Mato Grosso, Brazil, using satellite-derived indices. *Applied Geography*, 32(2), 702-713.
<http://dx.doi.org/10.1016/j.apgeog.2011.08.007>
- Brazil.org.za,. (2016). Mato Grosso. Retrieved 18 February 2016, from <http://www.brazil.org.za/mato-grosso.html>
- Ce.utexas.edu,. (2016). Retrieved 18 February 2016, from
<http://www.ce.utexas.edu/prof/maidment/giswr2010/Ex6/EX6.htm>
- Curtin, K. (2007). Network Analysis in Geographic Information Science: Review, Assessment, and Projections. *Cartography and Geographic Information Science*, 34(2), 103-111. <http://dx.doi.org/10.1559/152304007781002163>
- Fearnside, P. (1982). DEFORESTATION IN THE BRAZILIAN AMAZON: HOW FAST IS IT OCCURRING?. *Interciencia*, 7(2), 82-85.
- Fearnside, P. (2003). Deforestation Control in Mato Grosso: A New Model for Slowing the Loss of Brazil's Amazon Forest. *AMBIO: A Journal Of The Human Environment*, 32(5), 343. [http://dx.doi.org/10.1639/0044-7447\(2003\)032\[0343:dcimga\]2.0.co;2](http://dx.doi.org/10.1639/0044-7447(2003)032[0343:dcimga]2.0.co;2)
- Gibson, P., & Power, C. (2000). *Introductory remote sensing*. London: Routledge.
- GIS Resources,. (2014). Why does NDVI, NDBI, NDWI Ranges From -1 to 1? - GIS Resources. Retrieved 18 February 2016, from <http://www.gisresources.com/ndvi-ndbi-ndwi-ranges-1-1/>
- Hall, G., Wang, F., & Subaryono,. (1992). Comparison of Boolean and fuzzy classification methods in land suitability analysis by using geographical information systems. *Environment And Planning A*, 24(4), 497-516.
<http://dx.doi.org/10.1068/a240497>
- Indiana, U. (2007). Land-use Decision Making, Uncertainty and Effectiveness of Land Reform in Acre, Brazilian Amazon. ProQuest.
- Jennings, N. (2011). *A Python primer for ArcGIS®* (1st ed.). Lexington, KY.: CreateSpace.
- Kallali, H., Anane, M., Jellali, S., & Tarhouni, J. (2007). GIS-based multi-criteria analysis for potential wastewater aquifer recharge sites. *Desalination*, 215(1-3), 111-119. <http://dx.doi.org/10.1016/j.desal.2006.11.016>
- Latlong.net,. (2016). Pantanal, Mato Grosso, Brazil Map Lat Long Coordinates. Retrieved 18 February 2016, from <http://www.latlong.net/place/pantanal-mato-grosso-brazil-4113.html>
- Maurya, S. P., Ohri, A., & Mishra, S. (2015). Open Source GIS: A Review.
- Middleton, N. (2008). *The global casino*. London: Hodder.
- Recycle More offers advice for recycling at home, school and at work. (2016). Recycle-more.co.uk.. Retrieved 15 December 2016, from <http://www.recycle-more.co.uk>.
- Richards, P., Pellegrina, H., VanWey, L., & Spera, S. (2015). Soybean Development: The Impact of a Decade of Agricultural Change on Urban and Economic Growth in Mato Grosso, Brazil. *PLOS ONE*, 10(4), e0122510.
<http://dx.doi.org/10.1371/journal.pone.0122510>
- Rikalovic, A., Cosic, I., & Lazarevic, D. (2014). GIS Based Multi-criteria Analysis for Industrial Site Selection. *Procedia Engineering*, 69, 1054-1063. <http://dx.doi.org/10.1016/j.proeng.2014.03.090>
- Rybarczyk, G. & Wu, C. (2010). Bicycle facility planning using GIS and multi-criteria decision analysis. *Applied Geography*, 30(2), 282-293. <http://dx.doi.org/10.1016/j.apgeog.2009.08.005>

Topcon OS Series. (2013) (1st ed.). Tokyo. Retrieved from
http://www.topcon.co.jp/en/positioning/products/pdf/OS_E.pdf

Watts, J. (2015). Amazon deforestation report is major setback for Brazil ahead of climate talks. The Guardian. Retrieved from <http://www.theguardian.com/world/2015/nov/27/amazon-deforestation-report-brazil-paris-climate-talks>

Zandbergen, P. (2014). Python scripting for ArcGIS® (1st ed.). Redlands: ESRI.

7.2 Images:

GIS Layers. (2016). Retrieved from <http://s3.amazonaws.com/libapps/accounts/85740/images/GISLayers.png>

University of Portsmouth,. (2016). University of Portsmouth Crest. Retrieved from <http://www.port.ac.uk/media/why-portsmouth/institution/institution-history-1990-1995.jpg>



UNIVERSITY *of* PORTSMOUTH

Practical Portfolio 2

An assessment of glacier flow dynamics and post-wildfire vegetation recovery



UP733160

Word Count: 1497

Contents

1.0 Tunabreen Glacier flow dynamics, Svalbard.....	2
1.1 Introduction.....	2
1.2 Terminus movement	3
1.3 Crevasse propagation	4
1.4 Further in site: Meltwater pools.....	4
2.0 Assessing Post-wildfire Vegetation Recovery	6
2.1 Introduction.....	6
2.2 Acquired datasets	6
2.3 Classified vegetation levels.....	7
2.4 Wildfire Impacts	9
3.0 References.....	10

Figures

Figure 1: Map showing Tunabreen terminus positon and distance measure points, across the observed years.....	2
Figure 2: Measured area change in Km ² between each ASTER image and net change for the whole time period.....	3
Figure 3: Overall distance travelled by glacier terminus over 2002 - 2010 period.	4
Figure 4: Glacial crevasses map for the time period, with values for assisting surge determination.....	5
Figure 5: View of LAS Dataset from ArcScene, 4 weeks post fire.....	6
Figure 6: View of LAS Dataset from ArcScene, 23 weeks post fire.....	6
Figure 7: View showing ground growth in the gully of the area at lower elevations.	6
Figure 8: Aerial view showing this increased growth above.	6
Figure 9: Plot showing vegetation recovery.	7
Figure 10: Comparison of the two LAS files from scans taken at week 4 and 23 post wildfire event.	8
Figure 11: Classified 3D view of week 4.	9
Figure 12: Classified 3D view of week 23.	9

Tables

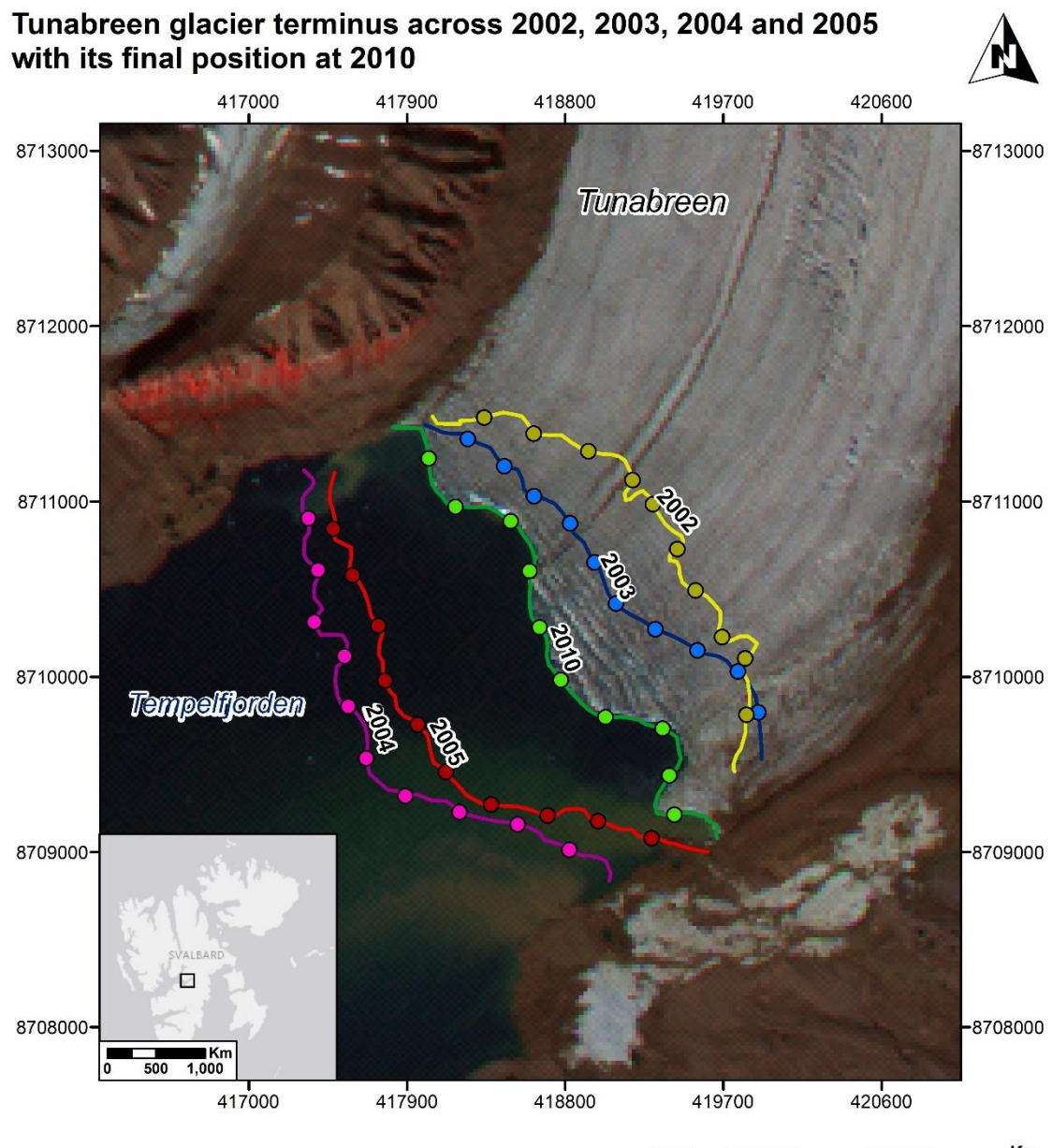
Table 1: The measured change of glacial position using both area and point distances.....	3
Table 2: Vegetation values of recovery for each type.....	7

1.0 Tunabreen Glacier flow dynamics, Svalbard

1.1 Introduction

Recent glacial melting is a positive feedback of annually increasing global temperatures due to climate change, yearly glaciers are in decline (ACIA, 2005; IPCC, 2014). A glacier's outlet is important, tidewater glacial melt has severe sea level rise impacts (Schannwell et al, 2016, p.161). Surging glaciers such as the tidewater Tunabreen glacier (Hodgkins and Dowdeswell, 1994, p.558) are thought to be advancing with little connection to climate variations, often they are intermittent between long periods of stagnation, the result is terminus progression (Flink et al, 2015, p.37). Described as cyclical by Murray (2003, p.14). Their fragile existence acts as an indicator of forecast climate change (Roer, 2008, p.8). This differentiation between surging and climate melt is key for a valid prediction of the effect climate change has upon glacier longevity (Flink et al, 2015, p.49).

Tunabreen glacier terminus across 2002, 2003, 2004 and 2005 with its final position at 2010



Features	Km	
2002 Terminus	0	0.2
2003 Terminus	0.4	0.6
2004 Terminus	0.8	1.0
2005 Terminus	1.2	1.4
2010 Terminus	1.6	1.8
2002 Distance points	Tunabreen	Glacier name
2003 Distance points	Tempelfjorden	Fjord name
2004 Distance points		
2005 Distance points		
2010 Distance points		

Figure 1: Map showing Tunabreen terminus position and distance measure points, across the observed years.

1.2 Terminus movement

Figure 1, shows the plotted terminus lines for the years stated, over a satellite image for 2010. Area difference between each year has been calculated from the digitised terminus lines. The change is shown in figure 2 graph, where an area increase shows a slight surge of 0.7488 km^2 with larger increase over the next year to 3.9922 km^2 for 2003 to 2004. This event can be classified as the surging event, while all subsequent change is a decrease, with a -0.7068 km^2 area reduction over the following year and a further reduction of -2.1689 km^2 over the next 5 years to 2010. The net change is shown in the last bar of figure 2 where overall the glacier increased across terminus area to 1.87 km^2 . However while this method is satisfactory for quantifying mass balance, it struggles to fully show, surging in the glacier centre.

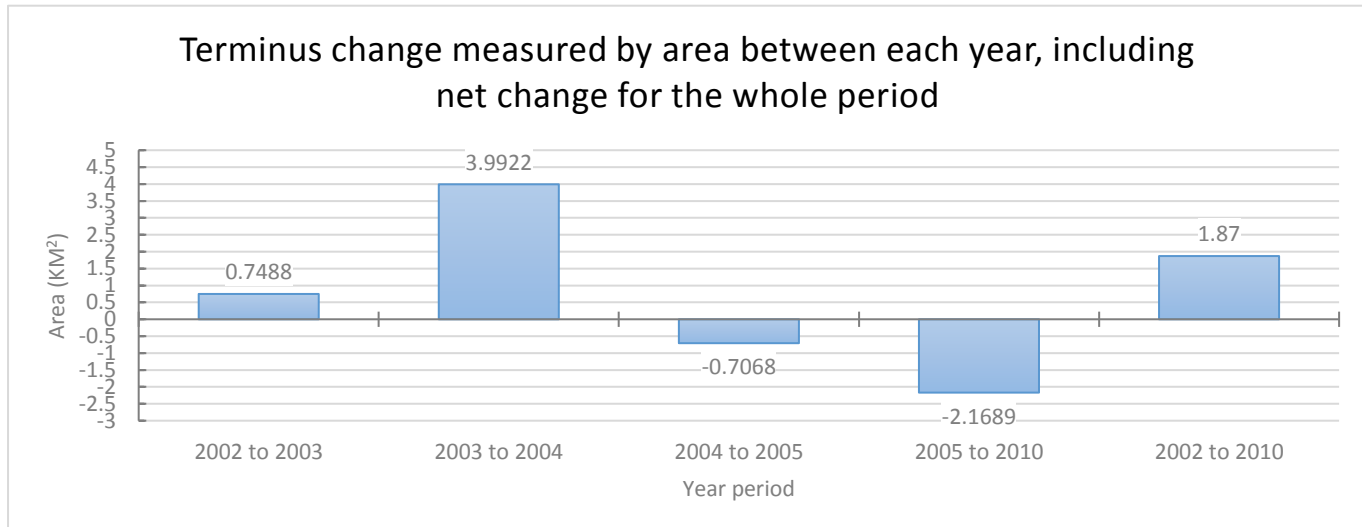


Figure 2: Measured area change in Km^2 between each ASTER image and net change for the whole time period.

Table 1 quantifies measurements taken from the ASTER images, the points on figure 1 show the distance points used for distance change measurement. Average distance change from each year showed 87% surge within 2003 to 2004 across the 2002 to 2004 surge period, similar to that of the terminus area change of 84% in the later surge year, with the decrease relationship being similar again. However it also serves to show the sectional glacier surging, where distance of net change for each point from 2002 to 2010 is plotted, central terminus movement is shown, where the edges move slower than the middle, this average rate of change can be calculated at 1.51 m/day for the whole period. This is as a result of friction from the valley edges, while the middle is under less opposing force (Benn and Evans, 2010, p.59).

Glacier year	2002 to 2003	2003 to 2004	2004 to 2005	2005 to 2010	2002 to 2010
Area change (Km^2)	0.75	3.99	-0.71	-2.17	1.87
Start point	65.50	735.02	-175.12	-419.06	206.34
1	153.73	1013.58	-152.96	-673.85	340.50
2	249.39	1214.16	-197.97	-703.65	561.93
3	401.44	1441.07	-364.04	-960.50	517.97
4	432.60	1490.96	-268.92	-1032.14	622.50
5	470.02	1624.63	-409.37	-888.01	797.27
6	467.17	1672.35	-459.24	-838.72	841.56
7	317.70	1712.33	-491.25	-819.44	719.34
8	159.43	1638.40	-501.85	-819.69	476.29
9	86.44	1526.62	-456.78	-483.41	672.87
10	-69.26	1330.20	-471.56	-189.21	600.17
End Point	-169.40	1109.91	-581.70	-95.07	263.74
Average (m)	213.73	1375.77	-377.56	-660.23	551.71
Max (m)	470.02	1712.33	-152.96	-95.07	841.56
Average rate of change (m/day)	0.59	3.77	-1.03	-1.81	1.51

Table 1: The measured change of glacial position using both area and point distances.

2002 to 2010 overall terminus distance difference (m)

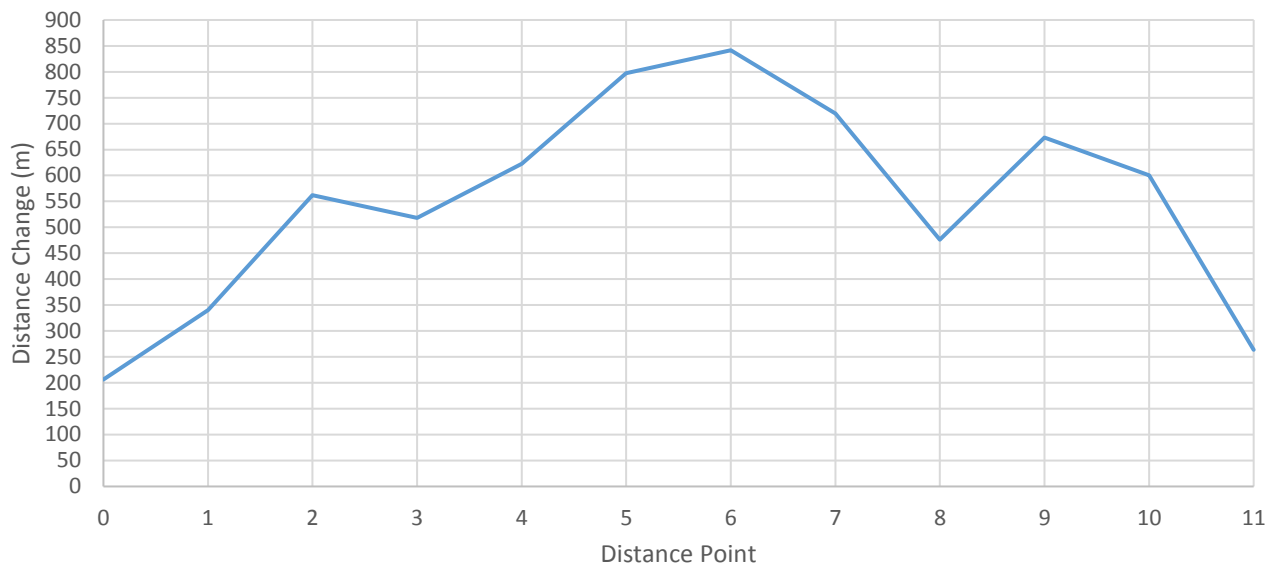


Figure 3: Overall distance travelled by glacier terminus over 2002 - 2010 period.

Figure 3 visualises the distance change for the whole period across the 10 distance points and the start and end of the terminuses. Surging across points 3 to 8 with a maximum around the centre at point 6 (841.56m) is represented, with the two lowest distances moved being at either end, directly meeting the valley edge, a frictional force.

While the reason behind glacial surging is unidentified, it is thought it may be due to either thermal or hydrological switch (Fowler et al, 2001; Van Pelt and Oerlemans, 2012; Sevestre and Benn, 2015). Where thermal switch is the result of thermal basal change with increasing temperatures at the base, this process has been recognised across Svalbard (Jiskoot, 2000). Hydrological switch the result of changes in hydrology at the glacier base (Benn and Evans, 2010, p.196).

1.3 Crevasse propagation

Figure 4 represents a comparison of mapped crevasses for ASTER images leading to the surge movement of 2005 and also in 2010. The total by 2005 is 745 crevasses with 71% of these found in the tail section the rest at the glacial front. From this maximum, the crevasse count decreased to 261 by 2010 with the majority (69%) found within the tail section and the rest found at the front. While the result of increased density of crevasses is due to surge events, the crevasses also tend to propagate further up the glacier, with the maximum distance of a crevasse from the terminus being 14.767 km in 2005, and a marked recovery of a 1.2km in 2010. These findings support the surge process, showing further propagation after surge events, with a recovery after deceleration. However such marked deceleration could be due to carving events at the terminus (Flink, 2013).

1.4 Further in site: Meltwater pools

Further assessment of the imagery, shows meltwater pools in figure 4, 2005. Research suggests that the 10 meltwater pools mapped may be as a result of Hydrological switch, whereby the build-up of hydrological pressure causes a release of water through onto the glacial surface, in the form of pools. It is thought that following these events, the rate of surging declines (Kamb, 1987). This theory is in line with the dynamic processes found, and hold a good basis for the explanation of the Tunabreen 2002 – 2005 surge event.

**Tunabreen glacier crevasses across the years 2002, 2003, 2004, 2005 and 2010,
showing pre surge and post surge activity**

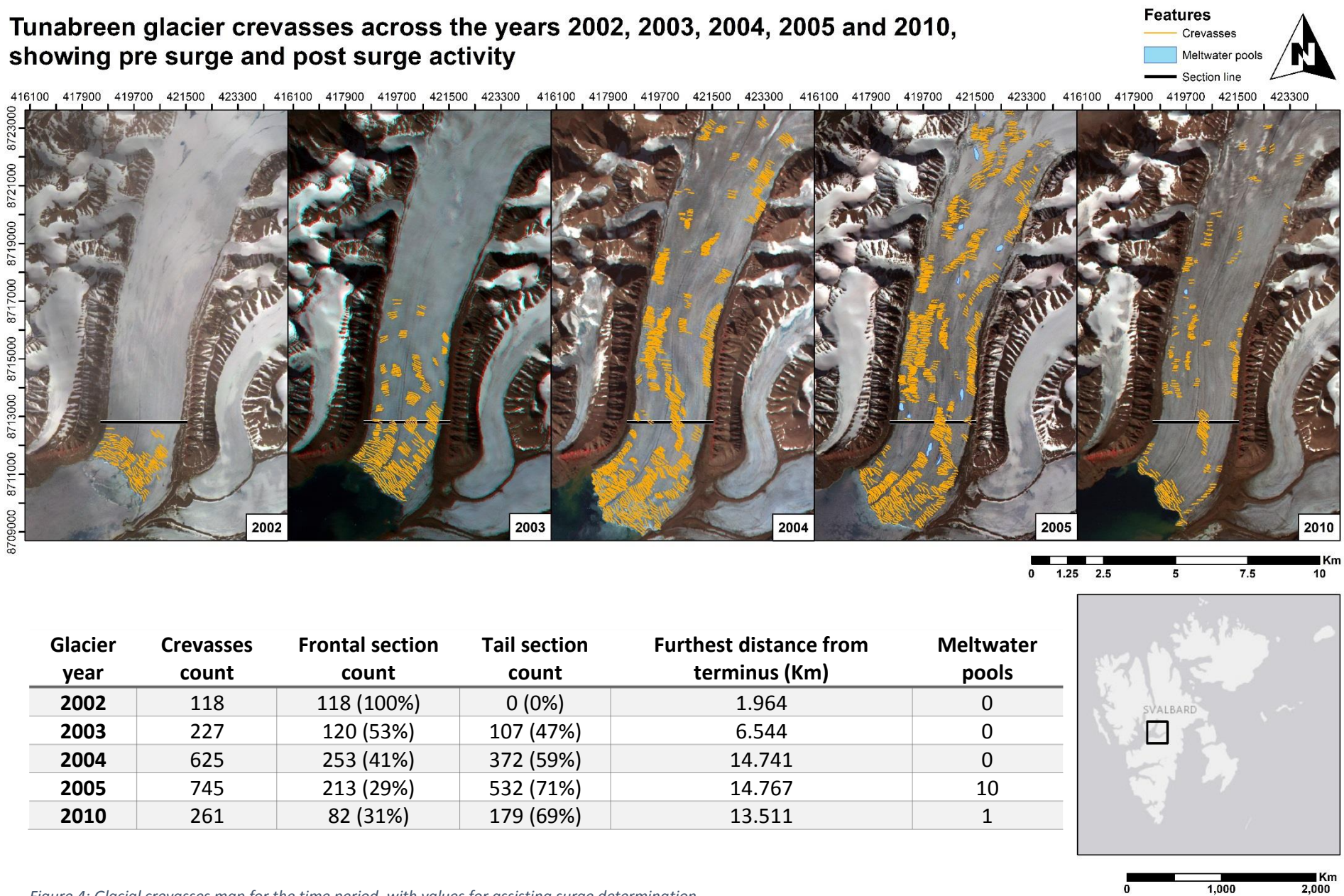


Figure 4: Glacial crevasses map for the time period, with values for assisting surge determination.

2.0 Assessing Post-wildfire Vegetation Recovery

2.1 Introduction

The current global temperature trends are resulting in an ever warmer climate, this is no exception for the UK. As this scenario continues an increased risk of wildfire is subsequent (Albertson et al, 2009, p. 2642). While the cause of wildfire is either natural – unavoidable – or due to human actions, it is the outcome and subsequent recovery that is predominant in research with the aim to encourage area rehabilitation. Maltby et al (1990) highlights the destruction wildfire can result in, for both ecosystems and vegetation. Taking Maltby et al's large scale study from the 600 ha area of North York moorland, further study can be applied to St Catherine's Hill, Christchurch. The area of Dorset, 6 miles North-East of Bournemouth, was subject to three fires burning over 70 ha (BBC, 2015). Point cloud LAS datasets provide a platform of which to classify vegetation and its week by week recovery, whilst also allowing statistical measurement (Rengers et al, 2016).

2.2 Acquired datasets

Below is the LAS datasets used, showing both 3D views and angled overlays.



Figure 5: View of LAS Dataset from ArcScene, 4 weeks post fire.



Figure 6: View of LAS Dataset from ArcScene, 23 weeks post fire.

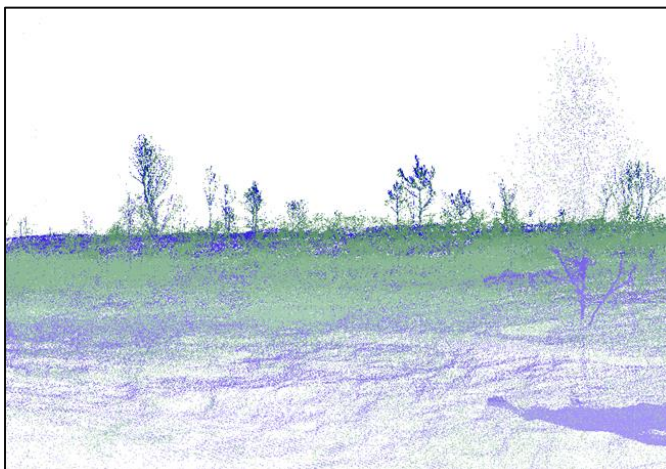


Figure 7: View showing ground growth in the gully of the area at lower elevations.

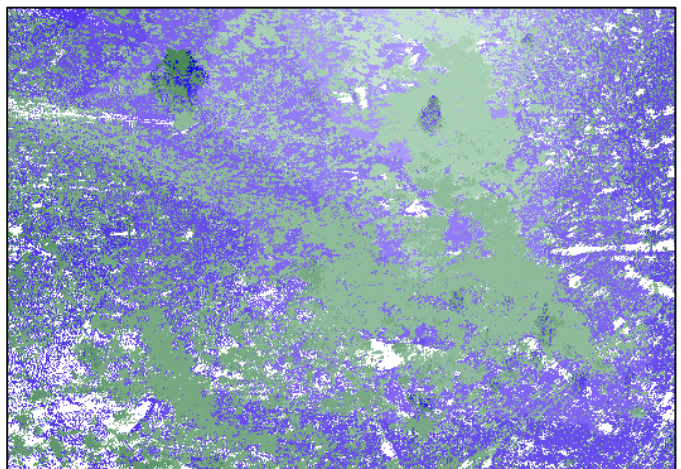


Figure 8: Aerial view showing this increased growth above.

2.3 Classified vegetation levels

Classification varied from low, medium and high vegetation, and scans processed were of 4 weeks post wildfire events and 19 weeks on at week 23. Total vegetation by week 4 was sparse at 4.57% as shown in figure 9. Over half of this value being comprised of low vegetation (2.52%), followed by medium vegetation (1.31%) and high vegetation (0.74%) as shown in table 2. The overall vegetation 19 weeks later was 40.33% as shown in figure 9. Just under 95% of this value comprised of low vegetation cover (38.16%), followed by medium (1.87%) and high vegetation (0.30%) as shown in table 2. While both low and medium vegetation increase by week 23, this is not true of high vegetation. High vegetation has shown a marked decrease by over 50% over the 19 weeks between the scans. This may be explained by tree carcasses visible in week 4, whereas by week 23 they had fallen to form low vegetation.

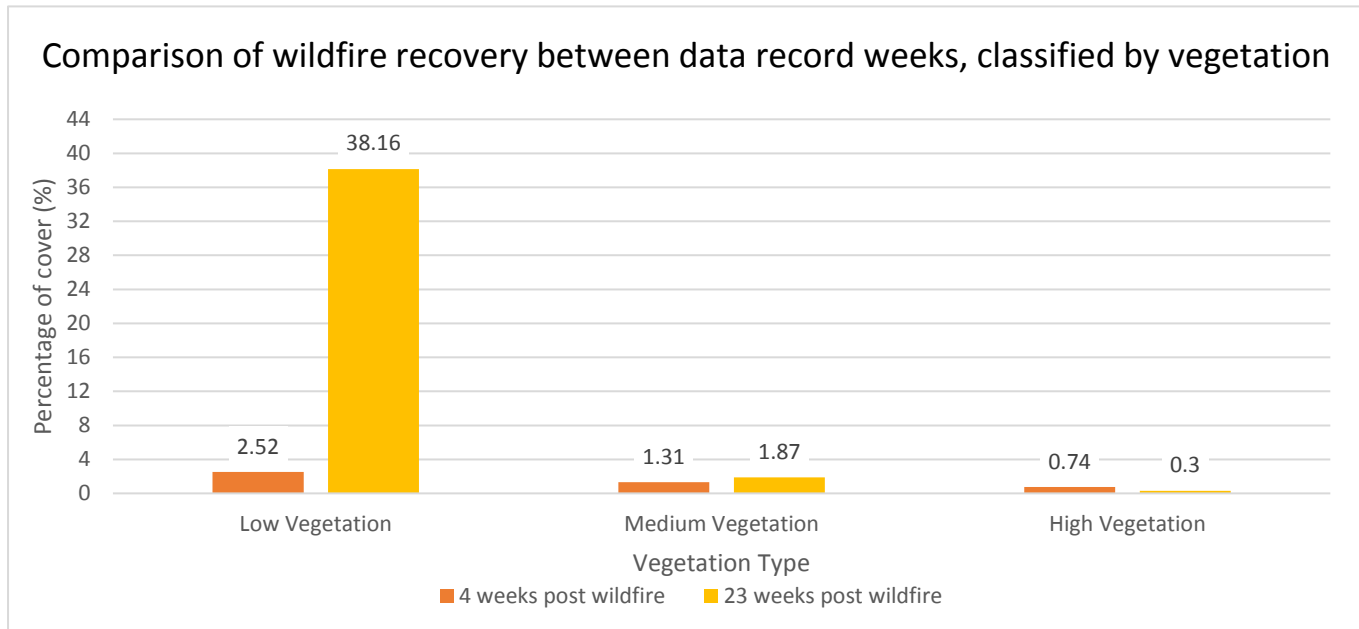


Figure 9: Plot showing vegetation recovery.

Forecasted rate of recovery is also shown in table 2, where values have been calculated from growth rates following the 19 week period from week 4 to week 23. It is estimated for low vegetation only that by week 28 it will be at 50% recovery with a prediction of 100% recovery by week 56. This has been further calculated for medium vegetation but shows extreme time periods, which resulted in further analysis of total vegetation recovery for all classes, where by week 27 vegetation will reach 50% recovery with a prediction of 100% recovery by week 54. While these values are good indicators, without knowing what vegetation coverage was for vegetation type prior to the wildfire event, it is unclear as to the final growth levels expected. However low vegetation, could be expected to reach 100%. Lastly high vegetation shows a deceleration of recovery, which is due to the length of time trees and megafauna take to develop, usually being in the 10's of years' time frame not weeks. Figure 10, 11, 12 show both a 2D and 3D representation of final vegetation classification.

	4 weeks post wildfire (%)	23 weeks post wildfire (%)	Rate of growth in first 4 weeks (%)	Rate of growth in 19 weeks since (%)	Forecast of 50% recovery following week 23 growth rates	Forecast of 100% recovery following week 23 growth rates
Low Vegetation (Grassland)	2.52	38.16	0.63	1.88	Week 28	Week 56
Medium Vegetation (Smaller shrubs and trees)	1.31	1.87	0.33	0.03	Week 1667	Week 3334
High Vegetation (Trees)	0.74	0.30	0.19	-0.023	n/a	n/a
Total Vegetation	4.57	40.33	1.14	1.88	Week 27	Week 54

Table 2: Vegetation values of recovery for each type.

A comparison of vegetation recovery after a wildfire event in St Catherines Hill, Christchurch, Dorset, UK

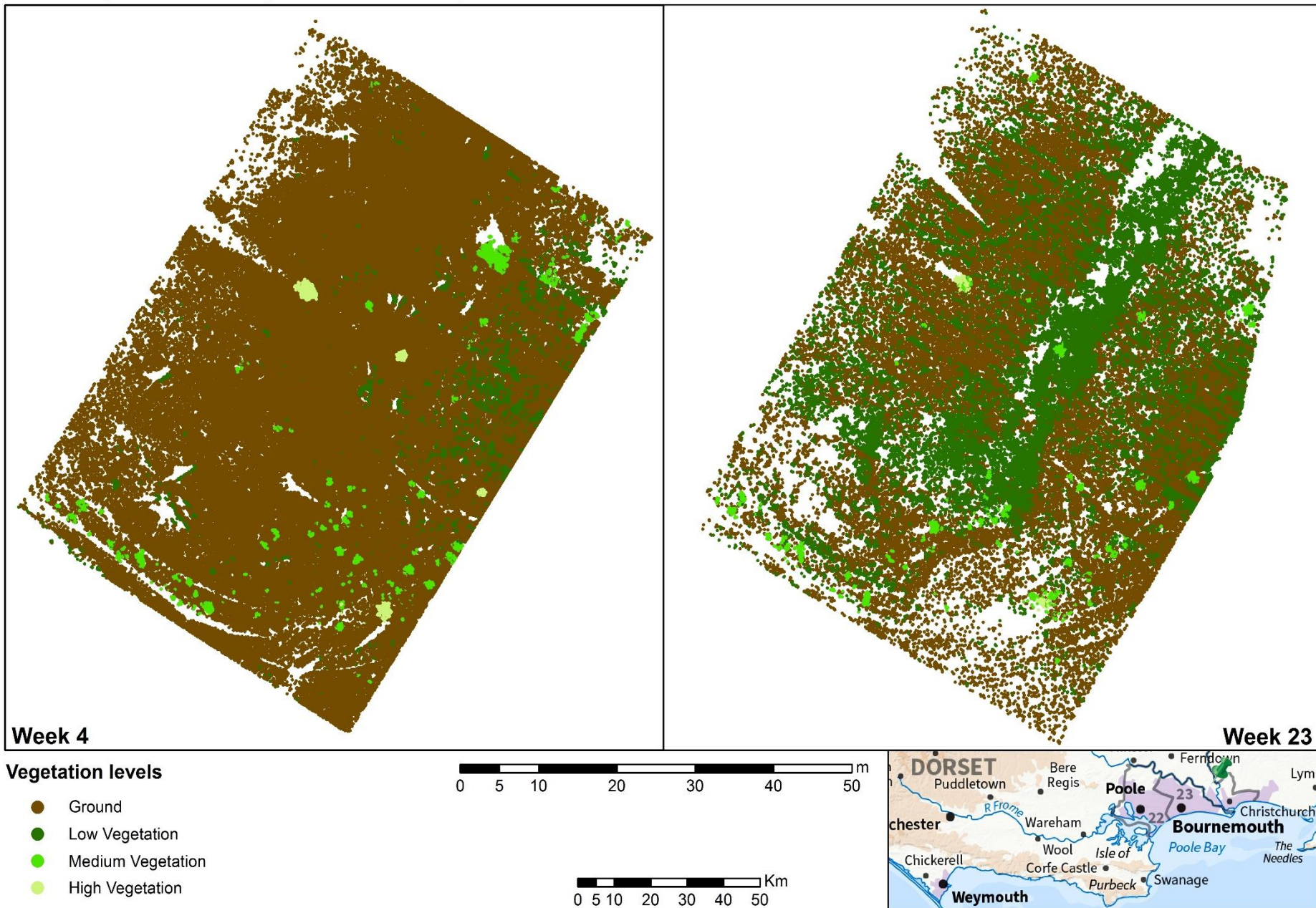


Figure 10: Comparison of the two LAS files from scans taken at week 4 and 23 post wildfire event.



Figure 11: Classified 3D view of week 4.

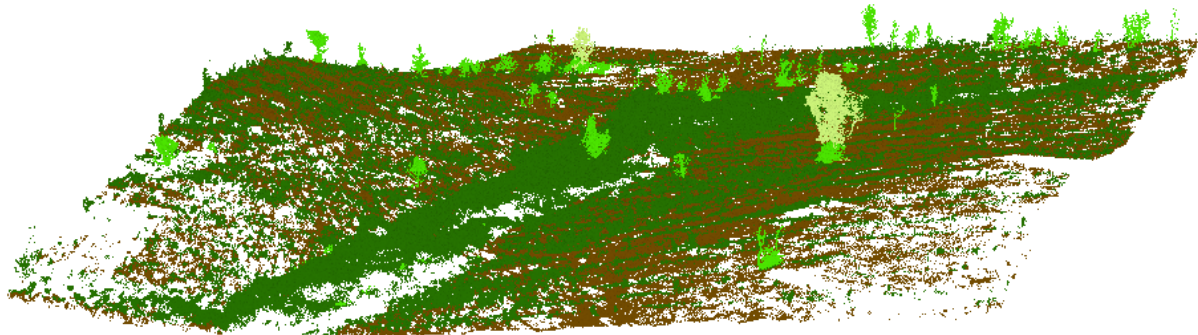


Figure 12: Classified 3D view of week 23.

2.4 Wildfire Impacts

The wildfire type can be considered a surface fire the largest impact was upon low vegetation. Surface fires may also evolve further upwards into crown fires, which would also account for the loss of high and medium vegetation (Scott, 1989). Vegetation variability is shown to react differently to wildfire events, while classifying vegetation as low, medium and high, micro changes within these classes are ignored. Bodi et al (2012) suggest the different resprouting ability of various flora, resulting in faster recovery, much like heathlands. Heathlands have shown remarkable capacity for recovery, even in the most severe fires according to Maltby et al (1990). Bodi et al (2012) further describes vegetation's ability to cope, by evolving fire-resistant seeds. However it is not always a discussion of recovery, many plants have shown to flourish in post wildfire ground (Bullock and Webb, 1995; Smith et al., 2009), where vital nutrients become abundant.

3.0 References

- ACIA (2005), Arctic Climate Impact Assessment, 1024 pp., Cambridge Univ. Press, New York.
- Albertson, K., Aylen, J., Cavan, G., & McMorrow, J. (2009). Forecasting the outbreak of moorland wildfires in the English Peak District. *Journal Of Environmental Management*, 90(8), 2642-2651.
- BBC (2015). Christchurch St Catherine's Hill fire 'deliberate'. BBC News website, accessed 25th January 2016. Retrieved from: <http://www.bbc.co.uk/news/uk-england-dorset-32136768>.
- Benn, D., & Evans, D. (2010). *Glaciers & glaciation* (2nd ed., p. 196). Routledge.
- Bodí, M. B., Cerdà, A., Mataix-Solera, J., & Doerr, S. H. (2012). A review of fire effects on vegetation and soil in the mediterranean basin. *Boletin de la asociacion de geografos espanoles*, (58).
- Bullock, J., & Webb, N. (1995). Responses to severe fires in heathland mosaics in Southern England. *Biological Conservation*, 73(3), 207-214.
- Flink, A. (2013). Dynamics of surging tidewater glaciers in Tempelfjorden, Spitsbergen (Masters). Stockholm University
- Flink, A., Noormets, R., Kirchner, N., Benn, D., Luckman, A., & Lovell, H. (2015). The evolution of a submarine landform record following recent and multiple surges of Tunabreen glacier, Svalbard. *Quaternary Science Reviews*, 108, 37-50.
- Fowler, A., Murray, T., & Ng, F. (2001). Thermally controlled glacier surging. *Journal Of Glaciology*, 47(159), 527-538.
- Hodgkins, R., & Dowdeswell, J. (1994). Tectonic processes in Svalbard tide-water glacier surges: evidence from structural glaciology. *Journal Of Glaciology*, 40(136), 553-560.
- Jiskoot, H., Murray, T., & Boyle, P. (2000). Controls on the distribution of surge-type glaciers in Svalbard. *Journal Of Glaciology*, 46(154), 412-422.
- Kamb, B. (1987). Glacier surge mechanism based on linked cavity configuration of the basal water conduit system. *Journal Of Geophysical Research*, 92(B9), 9083. <http://dx.doi.org/10.1029/jb092ib09p09083>
- Maltby, E., Legg, C., & Proctor, M. (1990). The Ecology of Severe Moorland Fire on the North York Moors: Effects of the 1976 Fires, and Subsequent Surface and Vegetation Development. *The Journal Of Ecology*, 78(2), 490.
- Murray, T., Strozzi, T., Luckman, A., Jiskoot, H., & Christakos, P. (2003). Is there a single surge mechanism? Contrasts in dynamics between glacier surges in Svalbard and other regions. *Journal Of Geophysical Research: Solid Earth*, 108(B5).
- Rengers, F., Tucker, G., Moody, J., & Ebel, B. (2016). Illuminating wildfire erosion and deposition patterns with repeat terrestrial lidar. *Journal Of Geophysical Research: Earth Surface*, 121(3), 588-608.
- Roer, I. (2008). Global glacier changes: facts and figures. M. Zemp, & J. van Woerden (Eds.). UNEP/Earthprint.
- Schannwell, C., Barrand, N., & Radić, V. (2016). Future sea-level rise from tidewater and ice-shelf tributary glaciers of the Antarctic Peninsula. *Earth And Planetary Science Letters*, 453, 161-170.
- Scott, A. C. (1989). Observations on the nature and origin of fusain. *International Journal of Coal Geology*, 12(1-4), 443-475.
- Sevestre, H. (2015). Surge-type glaciers: controls, processes and distribution.
- Sevestre, H., & Benn, D. (2015). Climatic and geometric controls on the global distribution of surge-type glaciers: implications for a unifying model of surging. *Journal Of Glaciology*, 61(228), 646-662.
- Smith, D. M., Finch, D. M., Gunning, C., Jemison, R., & Kelly, J. F. (2009). Post-wildfire recovery of riparian vegetation during a period of water scarcity in the southwestern USA.
- Van Pelt, W., & Oerlemans, J. (2012). Numerical simulations of cyclic behaviour in the Parallel Ice Sheet Model (PISM). *Journal Of Glaciology*, 58(208), 347-360.